MOLECULAR AND CELLULAR BIOLOGY, Mar. 2009, p. 1249–1265 Vol. 29, No. 5
0270-7306/09/$08.00+0 doi:10.1128/MCB.00853-08

Activation of Stat3 by Heregulin/ErbB-2 through the Co-Option of Progesterone Receptor Signaling Drives Breast Cancer Growth▽†

Cecilia J. Proietti,‡ Cinthia Rosemblit,‡ Wendy Beguelin, Martín A. Rivas, María Celeste Díaz Flaqué, Eduardo H. Charreau, Roxana Schillaci, and Patricia V. Elizalde*

Instituto de Biología y Medicina Experimental, CONICET, Obligado 2490, Buenos Aires 1428, Argentina

Received 28 May 2008/Returned for modification 15 July 2008/Accepted 4 December 2008

Cross talk between the steroid hormone receptors for estrogen and progesterone (PR) and the ErbB family of receptor tyrosine kinases appears to be a hallmark of breast cancer growth, but its underlying mechanism remains poorly explored. Here we have highlighted signal transducer and activator of transcription 3 (Stat3) as a key protein activated by heregulin (HRG), a ligand of the ErbB receptors, through co-opted, ligand-independent PR function as a signaling molecule. Stat3 activation was an absolute requirement in HRG-induced mammary tumor growth, and targeting Stat3 effectively inhibited growth of breast cancer cells with activated HRG/ErbB-2 and PR. Our findings unravel a novel potential therapeutic intervention in PR- and ErbB-2-positive breast tumors, involving the specific blockage of PR signaling activity.

Accumulated evidence indicates that the ErbB family (epidermal growth factor receptor [EGFR]/ErbB-1, ErbB-2, ErbB-3, and ErbB-4) of receptor tyrosine kinases is involved in breast cancer growth. Particularly, ErbB-2 overexpression in breast tumor samples is associated with increased metastatic potential and a poor prognosis (34). A large number of ligands for ErbBs have been described, including all isoforms of heregulins (HRG), which bind to ErbB-3 and ErbB-4 and recognize EGFR and ErbB-2 as coreceptors (35). Although the molecular mechanisms through which ErbBs control breast cancer growth have yet to be elucidated fully, the activation of mitogenic intracellular signaling, such as the p42/p44 mitogen-activated protein kinase (MAPK) pathway, seems to be causally involved in ErbB-induced breast cancer proliferation (27). Notably, several research works, including our own with progesterone receptor (PR) and HRG (20), have demonstrated that unliganded steroid hormone receptors (SHR) could indeed be transcriptionally activated through cross talk with ErbB signaling pathways (22, 39), indicating that another likely mechanism through which ErbBs induce breast cancer proliferation is by ligand-independent activation of SHR. On the other hand, several reports as well as our own findings with HRG/ErbBs and PR have shown that steroid hormones are able to activate ErbBs in breast cancer (2, 9, 21). Bidirectional cross talk between steroid hormones and ErbB signaling pathways therefore seems to be a hallmark of mammary cancer growth.

Over the last few years, a unique family of proteins, the signal transducers and activators of transcription (Stats), were found to be involved in cross talk with both steroid hormones and ErbB receptors (30, 38). Particularly, accumulating evidence has revealed that one of the members of the Stat family, Stat3, plays a key role in breast tumorigenesis (38).

We already demonstrated that HRG, acting via ErbB-2, induced growth in C4HD cells from an experimental model of hormonal carcinogenesis in which the synthetic progestin medroxyprogesterone acetate (MPA) induced mammary adenocarcinomas in female BALB/c mice (2). Notably, we found that HRG proliferative effects in both C4HD cells (2) and the human breast cancer cell line T47D (20) required PR activation. Interestingly, our previous work has unraveled that ErbB-2 also plays a key role in C4HD and T47D cell growth stimulated by progestins (1), disclosing the bidirectional nature of the interaction between progestin/PR and HRG/ErbB-2. Finally, we have recently shown that progestins are able to induce Stat3 activation in C4HD and T47D cells (28) and that the presence of activated Stat3 is an absolute requirement for progestin/PR stimulation of breast cancer growth (28). In the present study, we explored whether Stat3 might be yet another player in the cross talk between PR and HRG/ErbBs that drives breast tumor growth. Our present findings demonstrate for the first time that HRG/ErbB-2 induces Stat3 activation in breast cancer cells through the co-option of PR signaling.

MATERIALS AND METHODS

Animals and tumors. Experiments were carried out with virgin female BALB/c mice raised at the Institute of Biology and Experimental Medicine of Buenos Aires. All animal studies were conducted as described previously (28). The C4HD tumor line expresses PR and estrogen receptor (ER) and lacks glucocorticoid receptor and EGFR/ErbB-1 expression (2, 20).

Antibodies. Antibodies to the following proteins were used: phosphotyrosine Stat3 (B-7), total Stat3 (C-20), phosphotyrosine Jak1 (Tyr1022/1023), total Jak1 (HR-785), total Jak2 (C-20), ErbB-2 (C-18), ErbB-2 (9G6), ErbB-3 (C-17), ErbB-4 (C-18), phosphotyrosine (PY99), phospho-p42/p44 MAPK (E-4), total p42/p44 MAPK (C-14), p85 regulatory subunit of phosphatidylinositol 3-kinase (Z-8), and retinoblastoma protein (C-15), all from Santa Cruz Biotechnology (Santa Cruz, CA); phosphotyrosine Src (Tyr 416), c-Src (36D10), phospho-ErbB2 (Tyr 1221/1222), phospho-ErbB-2 (Tyr 877), and phosphotyrosine Jak2 (Tyr 1007/1008), from Cell Signaling (Beverly, MA); hPR Ab-7 (clone 7), ErbB-4/HER-4 oncoprotein (Ab-2), phosphoserine 294 PR (Ab-12), and actin (clone

* Corresponding author. Mailing address: Laboratory of Molecular Mechanisms of Carcinogenesis, Instituto de Biología y Medicina Experimental (IBYME), Obligado 2490, Buenos Aires 1428, Argentina. Phone: 5411-4783-2869. Fax: 5411-4786-2564. E-mail: Elizalde@dna.uba.ar.

† Supplemental material for this article may be found at http://mcb.asm.org/.

‡ C.J.P. and C.R. contributed equally to this paper.

▽ Published ahead of print on 22 December 2008.

ACTN05), from Neomarkers (Freemont, CA); v-Src (Ab-1), from Calbiochem; and FLAG-M2 monoclonal antibody, from Sigma (St. Louis, MO).

Cell culture and treatments. Primary culture of epithelial cells from C4HD tumors was performed as previously described (1, 2, 20). Cells were incubated in the presence or absence of 20 ng/ml of recombinant human HRGβ1 (Neomarkers, Freemont, CA). When indicated, cells were pretreated for 90 min with RU486. To block c-Src, ErbB-2, and p42/p44 MAPK activation, cells were preincubated with 10 μM 4-amino-5-(4-chlorophenyl)-7-(*t*-butyl)pyrazolo[3,4-*d*]pyrimidine (PP2) (Calbiochem, San Diego, CA), 50 μM tyrphostin AG825 (Calbiochem), and 10 μM UO126 (Sigma, St. Louis, MO), respectively, for 90 min before the addition of HRG. In experiments in which ErbB-2 was blocked, cells were pretreated with 2 μM antisense oligodeoxynucleotides (ASODNs) to ErbB-2 mRNA or, as a control, with 2 μM sense oligodeoxynucleotides (SODNs) for 48 h before the addition of HRG. Sequences of ODNs have already been detailed (1). In experiments assessing the role of ErbB-3 or ErbB-4, cells were preincubated with either an ErbB-3 mouse monoclonal antibody (oncoprotein Ab-5, clone H3.105.5; Neomarkers) or an ErbB-4 mouse monoclonal antibody (oncoprotein Ab-3, clone H4.72.8; Neomarkers) prior to HRG treatment, as already described (20). As control, cells were also incubated with preimmune mouse serum. T47D and SK-BR-3 cells were obtained from the American Type Culture Collection. T47D-Y cells were a generous gift from K. Horwitz (University of Colorado Health Sciences Center, Denver, CO). In experiments assessing the effect of HRGs on Stat3 activity, T47D cells, T47D-Y cells, T47D-Y cells transfected with PR-expressing vectors, and SK-BR-3 cells were cultured in Dulbecco's modified Eagle's medium (without phenol red) supplemented with 0.1% charcoalized fetal calf serum (ChFCS) and subjected to the treatments described above for C4HD cells. Cell proliferation was evaluated by a [^{3}H]thymidine incorporation assay as previously described (28). Assays were performed in octuplicate, and differences between control and experimental groups were analyzed by analysis of variance followed by a Tukey *t* test between groups. In former experiments, we had demonstrated that thymidine uptake correlates with the number of cells/well (2).

Western blot analysis and immunoprecipitation assays. Lysates were prepared from cells subjected to the different treatments described in each experiment, as previously detailed, and proteins were subjected to sodium dodecyl sulfate-polyacrylamide gel electrophoresis (28). Proteins were electroblotted onto nitrocellulose, and membranes were immunoblotted with the indicated antibodies as described previously (28). c-Src activity was studied by immunoprecipitating 500 μg protein with anti-total-c-Src antibody and performing Western blotting with a phosphotyrosine 418/423 c-Src antibody. ErbB-2 activity was studied by immunoprecipitating 250 μg protein with an ErbB-2 antibody and revealing the blot with a phosphotyrosine (p-Tyr) antibody. The association among ErbB-2, c-Src, and Stat3 was studied by performing coimmunoprecipitation experiments. Total cell lysates (1 mg protein) were immunoprecipitated using either an ErbB-2 (C-18) or a Stat3 (C-20) antibody (both from Santa Cruz Biotechnology, Santa Cruz, CA). As a control for the specificity of the protein interaction, lysates were also immunoprecipitated with normal rabbit serum (NRS) and a transforming growth factor beta receptor II (TGF-βRII) antibody (L-21; Santa Cruz Biotechnology).

Preparation of nuclear and cytosolic extracts. The NE-PER nuclear and cytoplasmic extraction reagent technique (Pierce Biotechnology, IL) was used per the manufacturer's instructions.

siRNA transfections. Small interfering RNAs (siRNAs) targeting PR and Stat3 mRNAs were synthesized by Dharmacon, Inc. (Lafayatte, CO) (PRsiRNA antisense, 5′-AUAGGCGAGACUACAGACGUU-3′; Stat3siRNA#1 antisense, 5′-CAACUCAGGAAAUUUGACCUU-3′; Stat3siRNA#2 antisense, 5′-CAUUCCCACAUCUCUGCUCUU-3′; and Stat3siRNA#3 antisense, 5′-UUAUGAAACACCAACGUGGUU-3′). A nonsilencing siRNA oligonucleotide from Dharmacon which does not target any known mammalian genes was used as a negative control. Transfection of siRNA duplexes was performed by using the DharmaFECT transfection reagent following the manufacturer's directions, using 100 nmol of siRNA, for 3 days.

Transient and stable transfections. In experiments assessing the role of Jak1 and Jak2 in HRG-induced effects on Stat3, C4HD and T47D cells were transiently transfected with 2 μg of a dominant-negative (DN) Jak1 vector or with 2 μg of a DN Jak2 vector (26), kindly provided by O. Silvennoinen (Tampere University Hospital, Finland) via N. Hynes (Friedrich Miescher Institute, Basel, Switzerland). T47D-Y cells were transiently transfected with 2 μg of plasmid encoding wild-type human PR-B (kindly provided by K. Horwitz), human PR-A (a gift from D. Edwards, Baylor College of Medicine, Houston TX), an S294A mutant PR-B which harbors a point mutation in which Ser 294 has been replaced by alanine (T47D-Y-S294APR-B) (a gift from C. Lange, University of Minnesota Cancer Center, Minneapolis, MN) (32), or a mutant PR-B engineered to convert three key prolines (P422A, P423A, and P426A) to alanines (PR-BmPro), thus abolishing PR binding to all of the SH3 domains and inhibiting activation of c-Src family tyrosine kinases (5) (provided by D. Edwards). The Fugene 6 transfection reagent technique (Roche Biochemicals, Indianapolis, IN) was used in accordance with the manufacturer's instructions. Transfection efficiencies were evaluated using the pEGFP-N1 vector (BD Biosciences Clontech, Palo Alto, CA) and determined by the percentage of cells that exhibited green fluorescence 24 h after transfection. Green fluorescent protein was visualized by direct fluorescence imaging using a Nikon Eclipse E800 confocal laser microscopy system (Nikon Instruments, Inc., Melville, NY). Transfection efficiencies varied between 60 and 70% (28). To study the role of Stat3 in proliferation, C4HD cells were transiently transfected as described above for 48 h with 2 μg of a DN Stat3 expression vector, Stat3Y705-F (6, 23), which carries a tyrosine-to-phenylalanine substitution at codon 705 that reduces phosphorylation on tyrosine of the wild-type Stat3 protein, therefore inhibiting both dimerization and DNA binding of Stat3 (7) (kindly provided by J. Darnell). As a control, cells were transfected with 2 μg of the empty pRc/CMV vector. Proliferation studies were done by also transfecting cells for 72 h with siRNAs. To investigate HRG's capacity to induce the transcriptional activation of Stat3, C4HD cells were transiently transfected with 2 μg of a luciferase reporter plasmid containing four copies of the m67 high-affinity binding site (7) and 10 ng of a *Renilla* luciferase expression plasmid, RL-CMV (Promega, Madison, WI), used to correct variations in transfection efficiency. In experiments assessing the role of Jaks in Stat3 transcriptional activation, cells were cotransfected with 2 μg DN Jak1 or 2 μg DN Jak2 expression vector. The total amount of transfected DNA was standardized by adding the pTATA-Luc reporter lacking the m67 insertion. Cells were then treated with HRG or preincubated with RU486, PP2, or ErbB-blocking antibodies for 90 min and then treated with HRG for 48 h, or they were left untreated. Transfected cells were lysed and luciferase assays carried out using a dual-luciferase reporter assay system (Promega). Duplicate samples were analyzed for each datum point. T47D-Luc cells were obtained by cotransfection of T47D cells with a Stat3 luciferase reporter plasmid containing four copies of the m67 high-affinity binding site (4×m67 pTATA TK-Luc) (7) and a neomycin resistance plasmid, using Fugene (Roche) according to the manufacturer's instructions, and selection with the neomycin analog G418 (Sigma) (500 μg/ml). Individual clones were propagated and screened for firefly luciferase activity, measured in total cell extracts according to the manufacturer's protocol (Promega, Madison, WI).

Immunofluorescence staining and confocal microscopy. C4HD cells grown on glass coverslips were incubated in medium with 0.1% ChFCS in the presence and absence of HRG (20 ng/ml) for 10 min. Cells were fixed and permeabilized in ice-cold methanol and were then blocked with phosphate-buffered saline–1% bovine serum albumin at room temperature. ErbB-2 was localized using either ErbB-2 C-18 or 9G-6 (Santa Cruz) antibody, and Stat3 was localized using a mouse monoclonal Stat3 antibody (124H6; Cell Signaling, Beverly, MA), followed by incubation with goat anti-rabbit immunoglobulin G–Alexa 488 (Molecular Probes, Eugene, OR) secondary antibody for ErbB-2 and with a rhodamine-conjugated anti-mouse secondary antibody (Jackson Laboratories) for Stat3. Stained cells were analyzed using a Nikon C1 confocal laser scanning microscope.

Cell cycle analysis. C4HD and T47D cells subjected to the different treatments described in Results were harvested for flow cytometric analysis and fixed in 70% ethanol for 24 h at 4°C. They were washed twice with phosphate-buffered saline, followed by RNA digestion (RNase A at 50 U/ml) and propidium iodide (PI) (20 μg/ml) staining for 30 min at room temperature in the dark. Cell cycle analysis was performed using a FACSCalibur flow cytometer (Becton Dickinson, Mountain View, CA) and Modfit LT software.

RESULTS

HRG induces Stat3 tyrosine phosphorylation through a mechanism requiring ErbB-2, ErbB-3, Jak1, Jak2, and c-Src activation. We performed the present study with primary cultures of C4HD murine mammary tumor epithelial cells and the T47D cell line. As we have already described, C4HD cells express high levels of PR, overexpress ErbB-2 and ErbB-3, and exhibit low ErbB-4 levels (2). Previous works have unraveled the capacity of anti-progestins to fully inhibit in vitro C4HD cell growth (13) as well as to abrogate in vivo C4HD tumor proliferation in syngeneic mice (33). We have also revealed Stat3 expression in C4HD cells (28). Our present findings showed that HRG treatment of C4HD cells induced strong

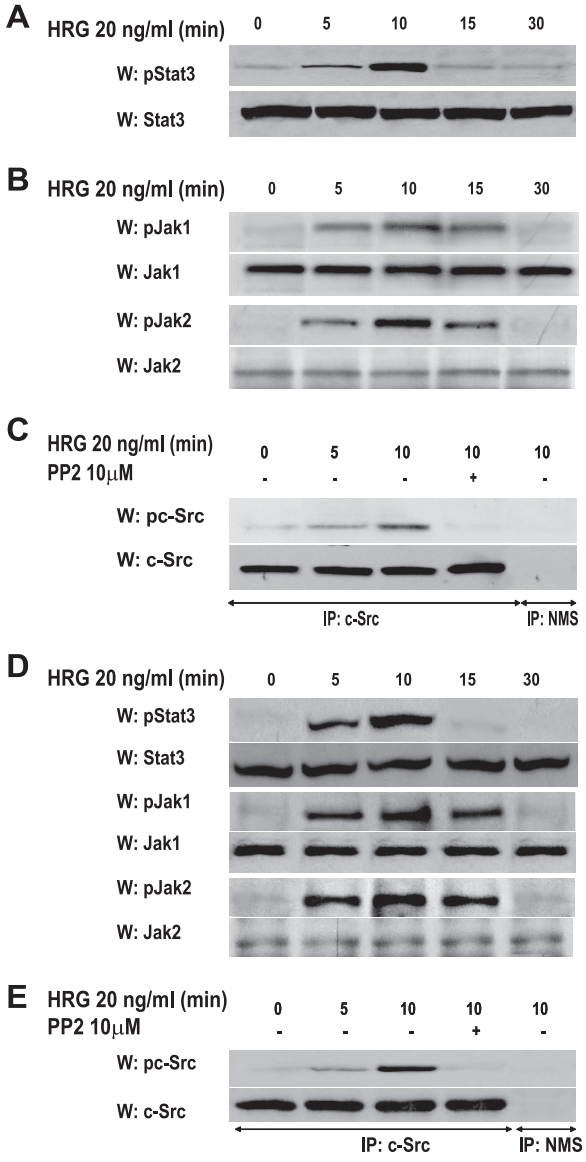

FIG. 1. HRG induces Stat3, Jak1, Jak2, and c-Src tyrosine phosphorylation. Cultures of C4HD (A to C) and T47D (D and E) cells were treated with HRG for the indicated times. Cell lysates (50 μg) were analyzed by Western blotting with phosphotyrosine 705 Stat3, phosphotyrosine 1022/1023 Jak1, and phosphotyrosine 1007/1008 Jak2 antibodies. Membranes were stripped and hybridized with total protein antibodies. c-Src activation was studied as described in Materials and Methods in cells treated and untreated with PP2 before HRG treatment. As a control, lysates were immunoprecipitated with normal mouse serum (NMS). Identical aliquots of each immunoprecipitate were subjected to immunoblot analysis with total c-Src antibody as a loading control. Phospho-protein bands underwent densitometry, and values were normalized to total protein bands. Data analysis showed that the increases in Stat3, Jak, and c-Src phosphorylation in cells treated for 10 min with HRG compared with the levels in untreated cells and the inhibition of HRG-induced c-Src phosphorylation levels caused by PP2 were significant ($P < 0.001$). Experiments shown were repeated five times with similar results. W, Western blot; IP, immunoprecipitation.

Stat3 phosphorylation on tyrosine 705 (threefold), whose highest level was observed at 10 min (Fig. 1A). HRG also stimulated tyrosine phosphorylation of two members of the Janus (Jak) family of soluble tyrosine kinases, Jak1 and Jak2 (Fig. 1B). We recently reported that C4HD cells express c-Src (28). Here we found that HRG treatment of C4HD cells for 10 min induced strong c-Src tyrosine (Tyr) 423 phosphorylation (Tyr 423 in the mouse protein corresponds to the orthologous Tyr 418 in the human protein), which was significantly inhibited by the selective Src family kinase inhibitor PP2 (Fig. 1C). Similar results were found in T47D cells, in which HRG induced Stat3, Jak, and Src tyrosine phosphorylation (Fig. 1D and E).

We then explored the participation of the different ErbB family members in HRG-induced Stat3 tyrosine phosphorylation. Figure 2A shows that Stat3 phosphorylation in C4HD cells was significantly inhibited by either blockage of ErbB-2 expression using ASODNs to its mRNA or preincubation with the specific ErbB-2 tyrosine kinase inhibitor AG825. We then investigated the roles of ErbB-3 and ErbB-4 by blocking HRG binding to these receptors by use of antibodies, as we previously described (20). As shown in Fig. 2A, abolishment of HRG binding to ErbB-3 with the blocking antibody Ab-5 inhibited HRG capacity to induce Stat3 tyrosine phosphorylation. In contrast, disruption of HRG binding to ErbB-4 with the Ab-3 antibody did not affect HRG-induced Stat3 phosphorylation, showing that ErbB-2/ErbB-3 is the functional heterodimer in HRG-induced Stat3 tyrosine phosphorylation (Fig. 2A). To investigate the involvement of Jaks in HRG-induced Stat3 phosphorylation, C4HD cells were transiently transfected with DN Jak1 or DN Jak2 vector (26) and then treated with HRG. Abolishment of Jak1 and Jak2 activity resulted in inhibition of HRG capacity to induce Stat3 tyrosine phosphorylation, evidencing that both kinases are involved in HRG effects (Fig. 2A). Finally, we found that inhibition of c-Src activity by preincubation of cells with PP2 also blocked HRG capacity to induce Stat3 phosphorylation (Fig. 2A). Similar mechanisms of HRG-induced Stat3 tyrosine phosphorylation were observed in T47D cells (Fig. 2A). Controls for the effects of AG825, the effects of the ErbB-3 and ErbB-4 monoclonal antibodies, the high efficiency of transfection of the DN Jak1 and Jak2 vectors, the effects and specificity of DN Jaks, and the specificity of ASODNs on ErbB-2 protein expression are shown in Fig. S1 in the supplemental material. The above results show that ErbB-2, Jaks, and Src all participate in HRG induction of Stat3 tyrosine phosphorylation. To gain further insight into the interplay among these proteins, we examined the tyrosine phosphorylation state of Jak1 and Jak2 in C4HD cells pretreated with PP2. We found that Jak1 and Jak2 tyrosine phosphorylation was effectively inhibited by PP2 (Fig. 2B, first and third panels, respectively). We also found that blockage of ErbB-2 tyrosine phosphorylation by AG825 abolished HRG capacity to activate Jak1 and Jak2 (Fig. 2B, first and third panels, respectively). Contrastingly, inhibition of Jak activity did not affect HRG capacity to induce Src phosphorylation (Fig. 2B, fifth panel) or ErbB-2 activation (data not shown). Comprehensively, our present findings indicate that by hierarchically directing Jak activation, c-Src and ErbB-2 mediate HRG-induced Stat3 tyrosine phosphorylation.

Assembly of a hierarchically activated multiprotein complex between ErbB-2, c-Src, and Stat3 in HRG-induced Stat3 tyrosine phosphorylation. While the capacity of ErbB-2 to associate with and activate Src is well acknowledged (19), c-Src function as an upstream regulator of ErbB-2 remains poorly studied (17, 18, 37). Therefore, we first explored the existence

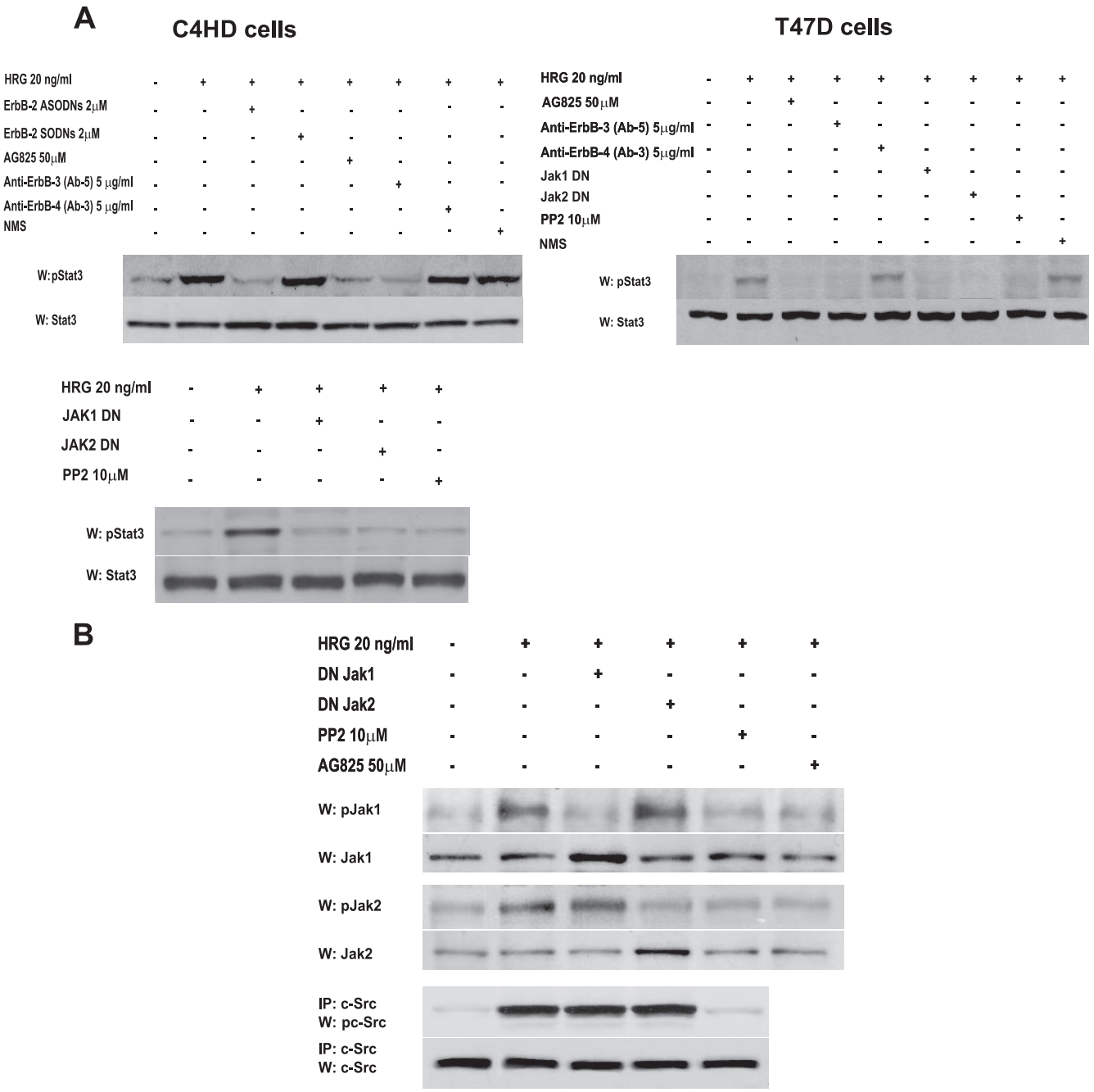

FIG. 2. Participation of ErbBs, Jaks, and c-Src in HRG-induced Stat3 phosphorylation. (A) C4HD (left) and T47D (right) cells were preincubated for 90 min with AG825, with monoclonal antibodies to either ErbB-3 or ErbB-4, and with normal mouse serum (NMS), transiently transfected with 2 μg of DN Jak1 or DN Jak2 vector for 2 days, and preincubated with PP2 for 90 min. C4HD cells were also pretreated for 48 h with either ASODNs or SODNs to ErbB-2. Cells were then treated with HRG for 10 min or left untreated. Fifty micrograms of protein from C4HD or T47D cell lysate was electrophoresed, and Western blots were performed with phosphotyrosine 705 Stat3 antibody. Membranes were stripped and hybridized with total Stat3 antibody. Phospho-Stat3 bands underwent densitometry, and values were normalized to total protein bands. Data analysis showed that the increase in Stat3 phosphorylation in cells treated with HRG compared with that in untreated cells and the inhibition of HRG-induced Stat3 phosphorylation levels by ErbB-2 ASODNs, AG825, ErbB-3 antibody, DN Jaks, and PP2 were significant ($P < 0.001$). These experiments were repeated five times with similar results. (B) Interplay among ErbB-2, Jaks, and Src. C4HD cells were preincubated with PP2 and AG825 or transiently transfected with 2 μg of DN Jak1 or DN Jak2 vector, as described for panel A, before treatment with HRG. Fifty micrograms of protein from cell lysates was immunoblotted with phosphotyrosine Jak1 and Jak2 antibodies. Membranes were stripped and hybridized with total Jak antibodies. c-Src activity in cell lysates was determined as described in the legend to Fig. 1. Phospho- and total Jak and c-Src bands underwent densitometry and were analyzed as detailed in the legend to Fig. 1, showing significant ($P< 0.001$) induction of Jak and c-Src phosphorylation by HRG and significant ($P < 0.001$) inhibition of HRG-induced Jak phosphorylation by PP2 and AG825. This experiment was repeated three times with similar results.

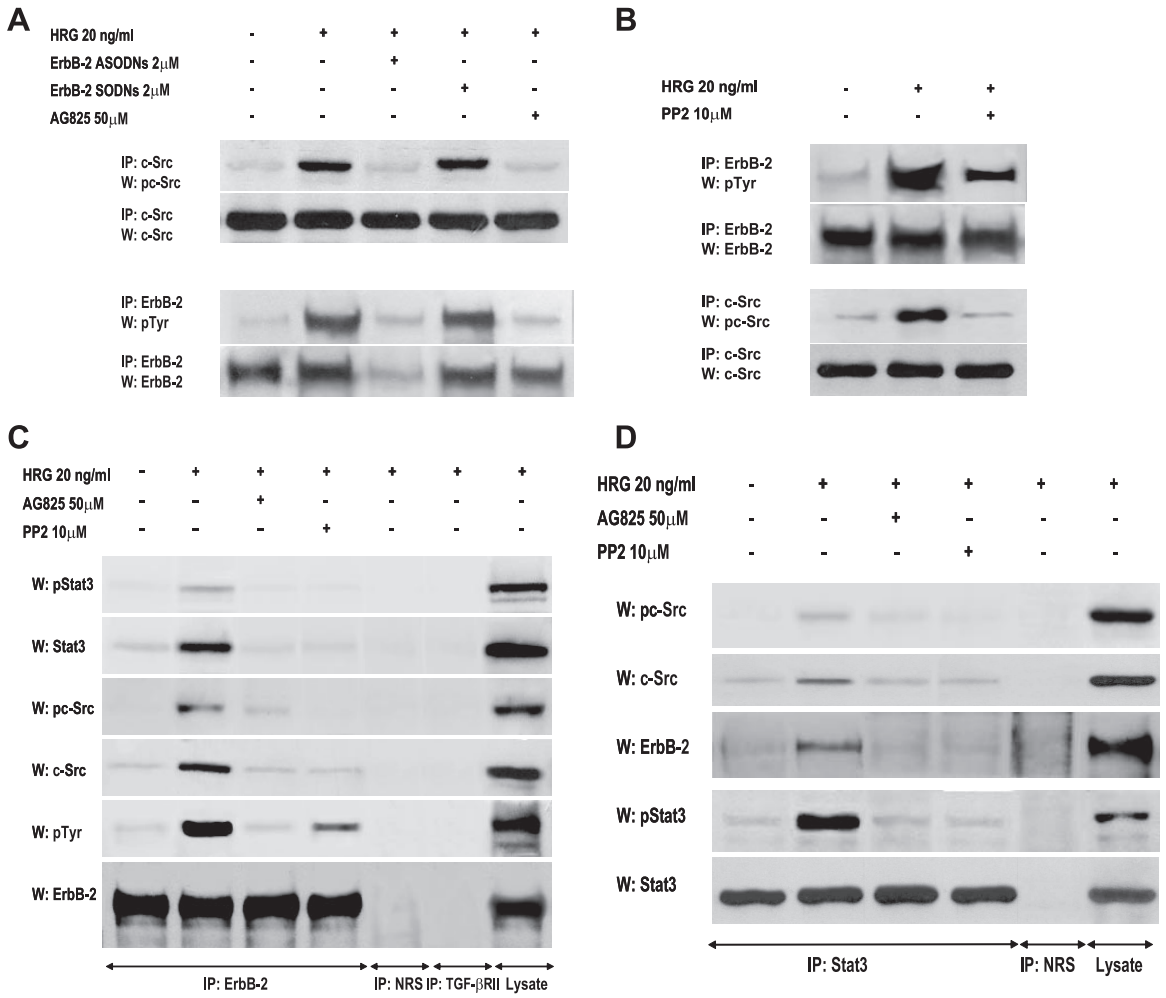

FIG. 3. HRG-induced interactions among ErbB-2, c-Src, and Stat3. (A and B) Interplay between ErbB-2 and c-Src in C4HD cells. (A) ErbB-2 expression and activation were blocked using ASODNs and AG825 respectively, as described in the legend to Fig. 2, and cells were treated with HRG for 10 min or left untreated. c-Src activity in cell lysates was determined as described in the legend to Fig. 1. ErbB-2 was immunoprecipitated from 250 μg protein with an ErbB-2 antibody, and the blot was revealed with a phosphotyrosine (p-Tyr) antibody. Identical aliquots of each immunoprecipitate were subjected to immunoblot analysis with the ErbB-2 antibody to verify that nearly equal amounts of immunoprecipitated proteins were loaded. Phospho-c-Src bands underwent densitometry, and values were normalized to total protein bands, showing that the increase in c-Src phosphorylation levels by HRG compared with those in untreated cells and the inhibition of HRG-induced c-Src phosphorylation by ErbB-2 ASODNs or AG825 were significant ($P < 0.001$). (B) Protein extracts from cells preincubated with PP2 before HRG treatment were analyzed for ErbB-2 and c-Src activation as described for panel A Phosphotyrosine bands in ErbB-2-immunoprecipitated extracts underwent densitometry and were normalized to total ErbB-2 bands, showing a significant ($P < 0.001$) increase in ErbB-2 phosphorylation levels by HRG and significant ($P < 0.001$) inhibition of HRG-induced ErbB-2 phosphorylation by PP2. The experiments shown in panels A and B were repeated three times with similar results. (C and D) Association among ErbB-2, c-Src, and Stat3. (C) Protein extracts (1 mg) from C4HD cells preincubated with AG825 or PP2 before HRG stimulation were immunoprecipitated with an ErbB-2 antibody and analyzed by Western blotting with phosphotyrosine 705 Stat3, phosphotyrosine 418/423 c-Src, total phosphotyrosine, and ErbB-2 antibodies. Membranes were then stripped and revealed with total Stat3, c-Src, and ErbB-2 antibodies. As controls for the specificity of the protein interactions, lysates were also immunoprecipitated with NRS and with TGF-βRII antibody. Cell lysates were blotted in parallel using the indicated antibodies. (D) C4HD protein extracts (1 mg) treated as described for panel C were immunoprecipitated with a Stat3 antibody and analyzed by Western blotting with phosphotyrosine 418/423 c-Src, ErbB-2, and phosphotyrosine 705 Stat3 antibodies. Membranes were then stripped and revealed with total c-Src and Stat3 antibodies. As a control, lysates were also immunoprecipitated with NRS. Cell lysates were blotted in parallel, using the indicated antibodies. The experiments shown in panels C and D were repeated three times with similar results.

of an interplay between ErbB-2 and c-Src in the mechanism of HRG-induced activation of both kinases. As shown in Fig. 3A, blockage of ErbB-2 expression by ASODNs to its mRNA or preincubation with AG825 resulted in significant inhibition of HRG-induced c-Src phosphorylation in C4HD cells. On the other hand, we found that inhibition of c-Src activity by PP2 significantly reduced HRG-induced ErbB-2 tyrosine phosphorylation, clearly showing that c-Src plays a role as an upstream ErbB-2 activator (Fig. 3B). We then explored whether a multimeric protein complex was assembled in the mechanism of HRG induction of Stat3 tyrosine phosphorylation. The physical association among proteins was explored by performing coimmunoprecipitation experiments. First, whole-cell protein extracts from C4HD cells treated and untreated with HRG for

10 min were immunoprecipitated with an anti-ErbB-2 antibody and immunoblotted with an anti-Stat3 antibody. As shown in Fig. 3C, we observed a weak basal association between ErbB-2 and Stat3. HRG treatment for 10 min induced a strong association between ErbB-2 and Stat3, which was abolished by inhibition of ErbB-2 phosphorylation with AG825 (Fig. 3C). In addition, we found that HRG caused an association between the phosphorylated forms of these proteins (Fig. 3C). As expected, since inhibition of ErbB-2 activity resulted in abolishment of Stat3 phosphorylation on tyrosine 705, no association between phospho-Stat3 and ErbB-2 was observed in the presence of AG825 (Fig. 3C). In the same protein complex, HRG increased the ErbB-2 and c-Src physical association, which was inhibited in the presence of PP2 (Fig. 3C). Interaction between phosphorylated c-Src and ErbB-2 was also evident upon HRG stimulation (Fig. 3C). Furthermore, as a consequence of the interplay between ErbB-2 and c-Src shown in Fig. 3A and B, inhibition of c-Src activity resulted in the abolishment of ErbB-2 association with either total Stat3 or phospho-Stat3, and conversely, inhibition of ErbB-2 activity inhibited total c-Src and phospho-c-Src association with Stat3 (Fig. 3C). As a control for the specificity of the interaction, we immunoprecipitated cell lysates with an antibody against TGF-βRII, a cell surface receptor which belongs to the family of transmembrane serine/threonine kinases, and with NRS. When protein extracts were immunoprecipitated with an anti-Stat3 antibody, HRG was also readily observed to induce physical interaction between the phosphorylated forms of Stat3 and c-Src and between total Stat3 and c-Src (Fig. 3D). In addition, we observed Stat3 and phosphorylated Stat3 physical interaction with ErbB-2 upon HRG stimulation (Fig. 3D). Taken together, our findings shown in Fig. 3C and D demonstrate that HRG stimulates the formation of a protein complex among ErbB-2, c-Src, and Stat3 in C4HD cells. In order to assess whether assembly of this complex was a common pathway in HRG-induced Stat3 activation in breast cancer, we performed similar studies with T47D cells. As shown in Fig. S2A and B in the supplemental material, physical interaction between Stat3, c-Src, and ErbB-2 was also induced by HRG in T47D cells. In addition, confocal microscopy studies with C4HD cells revealed that after 10 min of treatment, HRG induced ErbB-2 migration to the cytoplasm (Fig. 4A, first row, lower panel), in accordance with recent studies of cells overexpressing ErbB-2 (36). Antibodies against the carboxyl (Fig. 4A) and the amino (not shown) ErbB-2 termini yielded the same results, evidencing full-length ErbB-2 cytoplasmic localization. Notably, this is the first report of ligand-induced translocation of ErbB-2 to the cytoplasm. Migration of Stat3 to the nucleus upon 10 min of HRG treatment was also readily detected. Furthermore, our finding evidenced a clear ErbB-2 colocalization with Stat3 in the cytoplasmic compartment after HRG stimulation (Fig. 4A, third row, lower panel). We also performed subcellular fractionation and immunoblotting studies that further confirmed HRG's capacity to induce ErbB-2 migration to the cytoplasm and Stat3 translocation to the nucleus after 10 min of stimulation of C4HD cells (Fig. 4B).

HRG induces Stat3 tyrosine phosphorylation through the co-option of PR signaling: role of c-Src activity as a nodal convergence point between HRG-mediated ErbB-2 and PR activation. Based on our previous findings that on the one hand HRG transactivates PR (20) and on the other hand PR induces Stat3 activation in breast cancer (28), we here explored whether PR might be yet another player in the mechanism of HRG-induced Stat3 tyrosine phosphorylation. We found that pretreatment of C4HD cells (Fig. 5A, first panel) with the progestin antagonist RU486 abolished HRG effects, clearly showing that PR is involved in Stat3 activation by HRG. The same results were obtained by knockdown of PR gene expression with PR siRNAs (Fig. 5A, first panel). Our findings with T47D cells also evidenced PR participation in HRG-induced Stat3 activation (see Fig. S3 in the supplemental material). In order to further explore the role of PR, we used PR-null T47D cells (T47D-Y), in which we found that HRG was no longer able to induce Stat3 tyrosine phosphorylation (Fig. 5B, first panel). However, when we transfected T47D-Y cells with wild-type human PR-B (T47D-Y-PR-B), HRG treatment resulted in strong Stat3 activation (Fig. 5B, first panel).

Our results evidenced that both c-Src and PR participate in HRG-induced Stat3 activation. Since PR has been found to activate c-Src in response to progestins (5, 25), we explored the PR role in c-Src activation induced by HRG. In our models with endogenous PR expression, PR siRNA (C4HD cells) and RU486 (C4HD and T47D cells) induced a significant but not complete inhibition of HRG capacity to phosphorylate c-Src (Fig. 5A; see Fig. S3 in the supplemental material). Typical experiments (Fig. 5A; see Fig. S3 in the supplemental material) indicated 60 to 70% inhibition of c-Src Tyr 418/423 phosphorylation by blockage of PR expression/activation. The results shown were obtained after 10 min of HRG stimulation at the highest levels of c-Src phosphorylation. After 2 min of treatment, we also observed a significant increase in HRG-induced c-Src phosphorylation that remained unaffected by pretreatment with RU486 in T47D and C4HD cells (not shown). Similar results were found by assessing c-Src kinase activity, using enolase as a substrate (data not shown). HRG was also able to induce detectable levels of c-Src Tyr 418 phosphorylation in PR-null T47D-Y and T47D-Y-PR-B cells (Fig. 5B, third panel). Levels of HRG-induced c-Src Tyr 418 phosphorylation after 10 min of treatment were significantly higher in T47D-Y-PR-B cells than in T47D-Y cells, confirming that although PR expression/activation is not an absolute requirement for HRG stimulation of c-Src phosphorylation, a stronger degree of c-Src phosphorylation is achieved through PR involvement. We previously found that HRG induced both PR-B and PR-A isoform phosphorylation on Ser 294 in C4HD and T47D cells (20) and that HRG-activated p42/p44 MAPKs are the kinases mediating this rapid phosphorylation of both PR isoforms (20). Therefore, we here assessed the role of PR phosphorylation on Ser 294 in HRG-induced Stat3 and c-Src activation. Blockage of HRG capacity to activate MAPKs with the specific MEK1/MEK2 inhibitor UO126 (Fig. 5A, fifth panel; see Fig. S3 in the supplemental material), which abolishes PR Ser 294 phosphorylation (Fig. 5A, seventh panel; see Fig. S3 in the supplemental material), resulted in inhibition of HRG-mediated Stat3 phosphorylation in C4HD (Fig. 5A, first panel) and T47D (see Fig. S3, first panel, in the supplemental material) cells and induced 50 to 60% abrogation of c-Src activation in both cell types (Fig. 5A, third panel; see Fig. S3 in the supplemental material). To further confirm the participation of Ser 294-phosphorylated PR in HRG-induced Stat3 activation, we

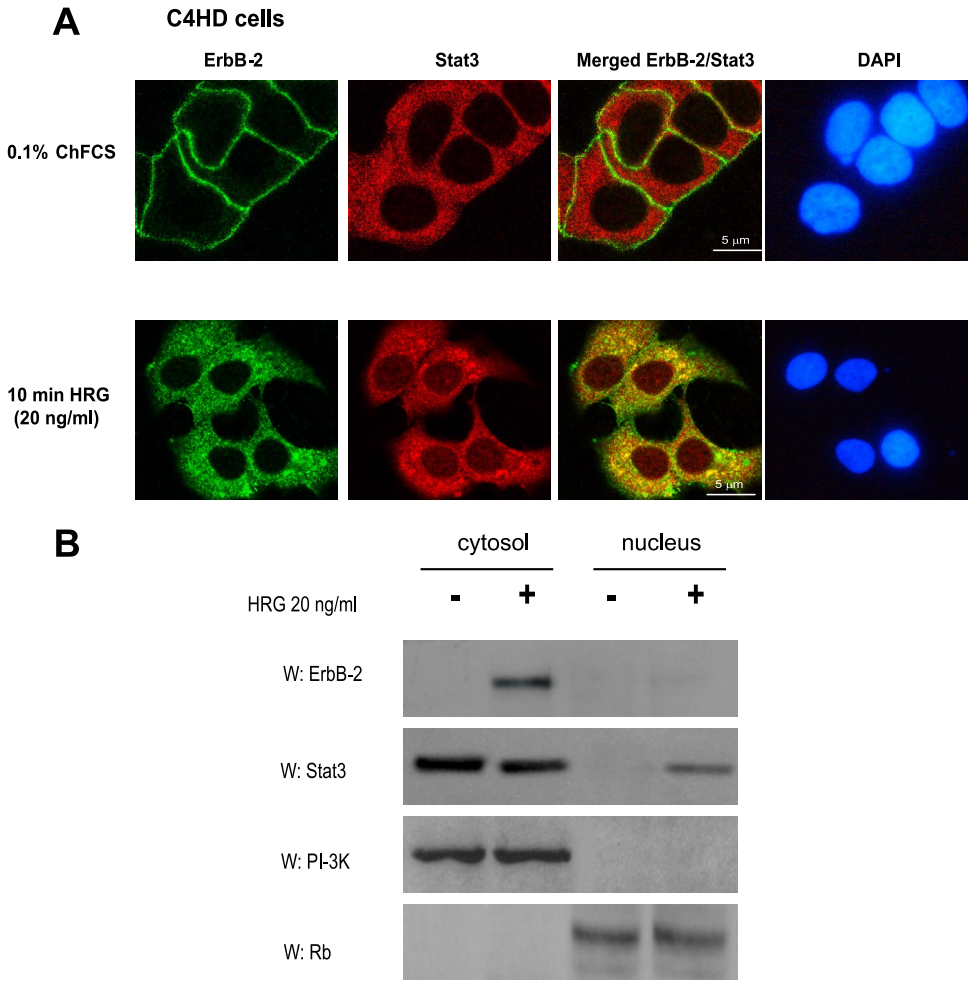

FIG. 4. HRG induces ErbB-2 and Stat3 cytoplasmic colocalization. (A) Cells were treated with HRG for 10 min or left untreated. ErbB-2 (green) and Stat3 (red) were localized as described in Materials and Methods. The same cells are shown in each row, and images in the right panel were formed by superimposition of images from the other two panels in the same row. Nuclei were stained with DAPI (4′,6-diamidino-2-phenylindole) (blue). HRG-induced colocalization of ErbB-2 and Stat3 is denoted by yellow coloration in the cytoplasm. The images are representative of three experiments. Bars, 5 μm. (B) C4HD cells were treated as described for panel A, and nuclear and cytosolic fractions were prepared. Fifty micrograms of protein from nuclear extracts and 25 μg protein from cytosolic extracts were analyzed by Western blotting for ErbB-2 and Stat3 expression. Membranes were then stripped and hybridized with an anti-p85 phosphatidylinositol 3-kinase (PI-3K) subunit antibody or an anti-retinoblastoma (Rb) antibody in order to control for cellular fractionation efficiency. W, Western blot. The data are representative of two experiments.

transfected T47D-Y cells with an S294A mutant PR-B which harbors a point mutation in which Ser 294 (T47D-Y-S294A-PR-B) has been replaced by alanine (32). As shown in Fig. 5B (first panel), HRG did not stimulate Stat3 tyrosine phosphorylation in T47D-Y-S294A-PR-B cells but was still able to activate c-Src to a significant extent in these cells (Fig. 5B, third panel). We also transfected T47D-Y cells with the mutant PR-BmPro, in which three prolines (P422A, P423A, and P427A) were converted to alanines (T47D-Y-PR-BmPro cells). Pioneering works defined the proline-rich domain of human PR as an absolute requirement for interaction with c-Src and consequent c-Src activation in response to progestins (5). While we did not find Stat3 tyrosine phosphorylation in response to HRG in T47D-Y-PR-BmPro cells (Fig. 5B, first panel), HRG capacity to induce c-Src phosphorylation was preserved (Fig. 5B, third panel). Interestingly, HRG induced detectable levels of PR phosphorylation on Ser 294 in T47D-Y-PR-BmPro cells (Fig. 5B, seventh panel), consistent with recent reports showing low levels of progestin-induced PR Ser 294 phosphorylation in T47D-Y cells stably expressing PR-BmPro (14). Our findings indicate that in spite of significant c-Src activation, phosphorylation of human PR at Ser 294 and the presence of an intact PR proline-rich domain are required by HRG to induce Stat3 activation in breast cancer cells. Further support of the PR role in full c-Src activation was provided by the demonstration that after 2 min of HRG treatment, levels of activated c-Src were similar in T47D, T47D-Y-PR-B, T47D-Y-S294A-PR-B, and T47D-Y-PR-BmPro cells, evidencing an early PR-independent c-Src activation (Fig. 5C). After 10 min of treatment, levels of c-Src phosphorylation in T47D-Y-PR-B cells were significantly higher than those after 2 min of treatment, but they remained unchanged in the other cell types

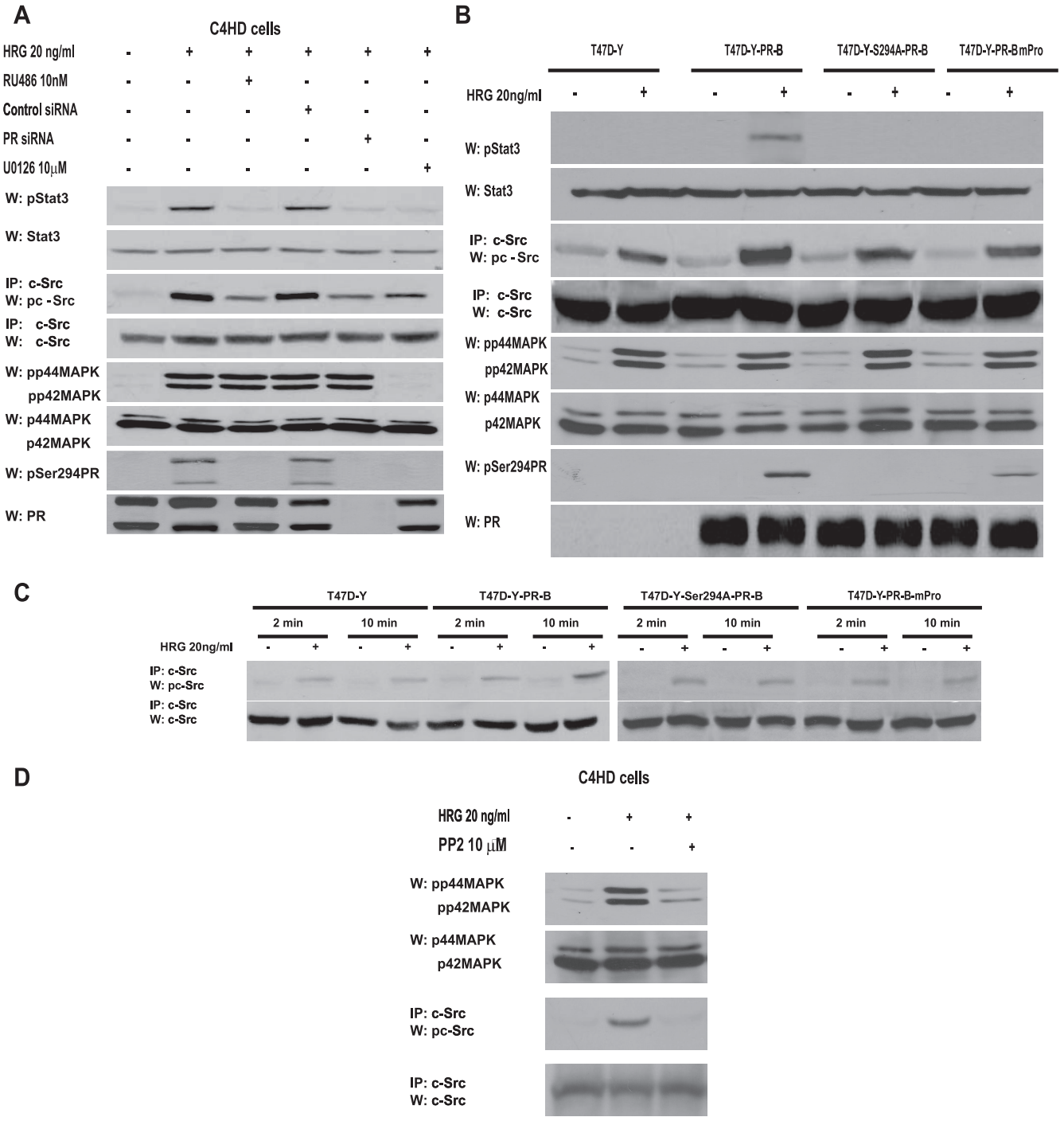

FIG. 5. HRG co-opts PR signaling to induce Stat3 activation. (A) C4HD cells were pretreated with RU486 or UO126 and were also transfected with specific PR or control siRNA before 10 min of HRG treatment. Cell extracts (50 μg protein) were electrophoresed, and Western blots were performed with the indicated phospho-protein antibodies. Filters were stripped and reprobed with the respective total protein antibodies. c-Src activity was studied as described in the legend to Fig. 1. Phospho-Stat3 and c-Src bands were subjected to densitometry and analyzed as described in the legend to Fig. 1, showing that inhibition of the HRG-induced Stat3 or c-Src phosphorylation level by RU486, PR siRNA, or UO126 was significant ($P < 0.001$). This experiment was repeated three times with similar results. (B) The indicated cells were treated with HRG or remained untreated. Stat3, c-Src, MAPK, and PR phosphorylation and differences in c-Src phosphorylation levels were determined as described for panel A. Data analysis showed that levels of c-Src phosphorylation in HRG-treated T47D-Y-PR-B cells were significantly higher than those in T47D-Y, T47D-Y-PR-BmPro, and T47D-Y-S294A-PR-B cells ($P < 0.001$). (C) T47D-Y cells transiently transfected with the indicated PR vectors were stimulated with HRG for the indicated times, and c-Src activation was studied as described in the legend to Fig. 1. (D) c-Src participates in HRG-induced MAPK activation. C4HD cells were preincubated with PP2 before 2 min of HRG treatment. Cell extracts (50 μg protein) were electrophoresed, and Western blots were performed with phospho-MAPK antibody. The filter was stripped and reprobed with total MAPK antibody. c-Src activity (third and fourth panels) was studied as described in the legend to Fig. 1.

(Fig. 5C). Our present findings also evidenced that the rapid, PR-independent HRG stimulation of c-Src activity participates in the mechanism of MAPK activation, since preincubation with PP2 significantly inhibited HRG-stimulated MAPK activation at 2 min of treatment in C4HD (Fig. 5D) and T47D (not shown) cells. Interestingly, HRG capacity to induce p42/p44 MAPK activation is independent of PR activity or expression, since neither RU486 in C4HD (Fig. 5A, fifth panel) or T47D (see Fig. S3, fifth panel, in the supplemental material) cells nor PR siRNAs in C4HD cells (Fig. 5A, fifth panel) abolished HRG stimulation of MAPK activity. This finding was further confirmed with T47D-Y cells, in which HRG capacity to induce MAPK activation remained unaffected in the absence of PR expression (Fig. 5B, fifth panel). Our results for T47D-Y-S294A-PR-B and T47D-Y-PR-BmPro cells (Fig. 5B, fifth panel) also evidenced that HRG-induced MAPK activation is independent of PR phosphorylation on Ser 294 and of the presence of an intact polyproline motif. The studies shown in Fig. 5A and B and in Fig. S3 in the supplemental material were done after 10 min of HRG treatment, at the time of highest HRG-induced Stat3 phosphorylation. However, it is notable that the highest levels of HRG-stimulated MAPK phosphorylation were reached after 2 min of treatment and were maintained for 15 min (data not shown).

Taking into account our findings that inhibition of PR activity significantly blocks c-Src activation in C4HD (Fig. 5A) and T47D (see Fig. S3 in the supplemental material) cells and, on the other hand, that blockage of c-Src activity results in decreased HRG-induced ErbB-2 phosphorylation (Fig. 3B), we reasoned that any strategy aimed at perturbing PR activation/phosphorylation at Ser 294 would in turn result in inhibition of HRG-induced ErbB-2 tyrosine phosphorylation. Indeed, our results evidenced that preincubation with RU486 or inhibition of PR phosphorylation on Ser 294 by abolishment of MAPK activity or PR siRNAs significantly reduced the levels of ErbB-2 tyrosine phosphorylation in C4HD cells (Fig. 6A), providing striking evidence that not only PR expression/activation but also PR phosphorylation on Ser 294 is required for HRG-induced ErbB-2 tyrosine phosphorylation. The same results were found with T47D cells (see Fig. S4A in the supplemental material). Most recently, it was shown that c-Src can act as an upstream activator of ErbB-2, promoting its phosphorylation on residue Tyr 877 (Tyr 927 in the mouse protein), a site different from the autophosphorylation sites and located in the activation loop of the kinase domain (17, 37). Therefore, we investigated the Tyr 877/927 phosphorylation state in our different model systems. As shown in Fig. 6B, HRG induced Tyr 877/927 ErbB-2 phosphorylation in C4HD cells, an effect that was completely blocked by PP2, evidencing c-Src involvement. Treatment of C4HD cells with RU486, knockdown of PR expression, or abolishment of PR Ser 294 phosphorylation with UO126 also resulted in inhibition of HRG-stimulated Tyr 877/927 ErbB-2 phosphorylation (Fig. 6B). Although diminished in the absence of c-Src activation by preincubation with PP2, HRG's capacity to phosphorylate a major autophosphorylation site of ErbB-2, Tyr 1222 (Tyr 1272 in the mouse protein), was notably still evident in C4HD cells (Fig. 6B). Furthermore, inhibition of PR activity with RU486 and blockage of PR Ser 294 phosphorylation with UO126 did not significantly affect HRG phosphorylation of ErbB-2 at Tyr 1222/1272 in C4HD cells (Fig. 6B). Figure S4B in the supplemental material illustrates a similar mechanism of HRG-induced ErbB-2 phosphorylation at Tyr 877 and Tyr 1222 in T47D cells. Taken together, our results indicate that HRG-induced phosphorylation of ErbB-2 on Tyr 877/927 occurs via c-Src and requires the presence of unliganded PR phosphorylated on Ser 294, with ErbB-2 Tyr 877/927 phosphorylation being the molecular event that couples HRG/ErbB-2 to Stat3 activation. To further explore the nature of the linkage between PR and c-Src leading to ErbB-2 phosphorylation on Tyr 877, we performed reconstitution experiments with T47D-Y cells. In the absence of PR expression, HRG was not able to induce ErbB-2 Tyr 877 phosphorylation (Fig. 6C). Contrastingly, HRG induced strong ErbB-2 Tyr 877 phosphorylation (8- to 10-fold) in T47D-Y-PR-B cells (Fig. 6C). In accordance with our findings for blocking PR phosphorylation on Ser 294 with UO126 (Fig. 6B), HRG capacity to induce Tyr 877 phosphorylation was impaired in T47D-Y-S294A-PR-B cells (Fig. 6C). In addition, HRG was not able to induce phosphorylation of ErbB-2 Tyr 877 in T47D-Y-PR-BmPro cells (Fig. 6C), providing additional evidence of the requirement of c-Src interaction with PR for this phosphorylation to occur. On the other hand, HRG induced phosphorylation of ErbB-2 at Tyr 1222/1272 in all four cell types (Fig. 6C). A ternary interaction among ErbB-2, PR, and c-Src upon HRG stimulation was also evidenced by coimmunoprecipitation analysis with C4HD and T47D cells (Fig. 6D). The presence of both PR-B and PR-A in this ternary complex was clearly detected (Fig. 6D). This was an expected result for T47D cells since the direct interaction of the polyproline motif, present in both human PR-B and PR-A isoforms, with the SH3 domain of c-Src has already been unraveled (3–5). Mouse PR lacks the polyproline motif, and therefore the association with c-Src seen in C4HD cells must be due to another regulatory modification of PR function induced by HRG. Our findings showing that Ser 294 phosphorylation of PR-B and PR-A is required for HRG-induced full levels of c-Src activation (Fig. 5A) prompted us to determine whether Ser 294 phosphorylation could mediate mouse PR-B and PR-A association with c-Src. We performed coimmunoprecipitation studies with C4HD cells in which PR Ser294 phosphorylation was abolished by preincubation with UO126. As shown in Fig. 6D, the association of PR-B, PR-A, and c-Src with ErbB-2 was strongly reduced in the absence of Ser 294 phosphorylation. Although PR-A capacity to activate cytoplasmic signaling remains poorly explored, pioneering findings evidenced human PR-A ability to activate Src kinases in cell-free assays (5). Interestingly, PR-A-induced Src and MAPK activation in response to progestin within cells was highly reduced compared to that induced by PR-B (3, 4). To address the role of PR-A in HRG-induced Stat3 activation, we transfected T47D-Y cells with a human PR-A expression vector (T47D-Y-PR-A). After 10 min of treatment, HRG was able to stimulate c-Src activation in T47D-Y-PR-A cells. However, levels of c-Src activation were significantly lower than those observed in T47D-Y-PR-B cells (Fig. 6E). Although strikingly reduced compared to that in T47D-Y-PR-B cells, HRG-induced Stat3 tyrosine phosphorylation was still observed in T47D-Y-PR-A cells (Fig. 6E). Similarly, we found impaired but clearly detectable phosphorylation of ErbB-2 Tyr 877 upon HRG stimulation in T47D-Y-PR-A cells with respect to T47D-PR-B cells (Fig. 6E). Con-

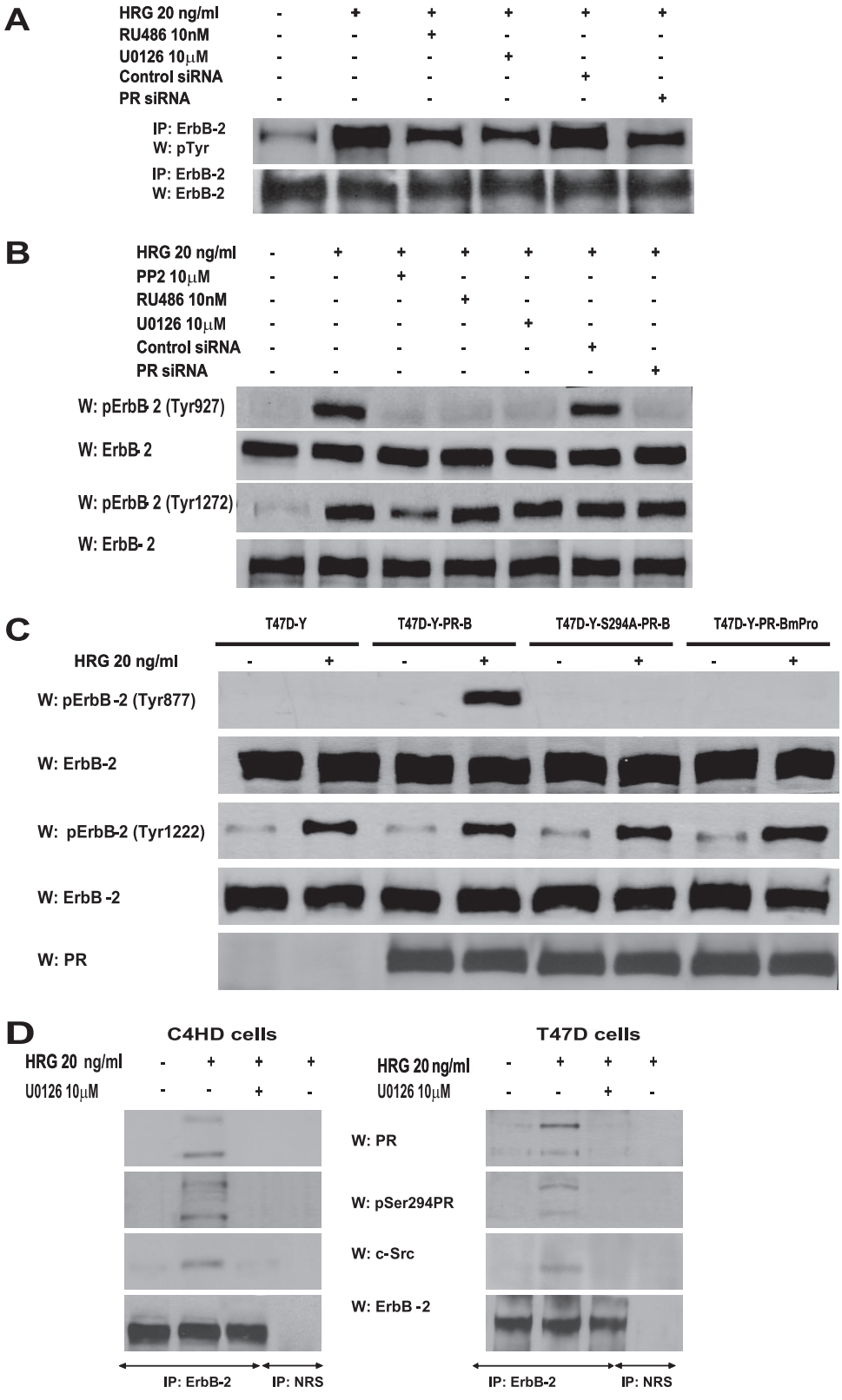

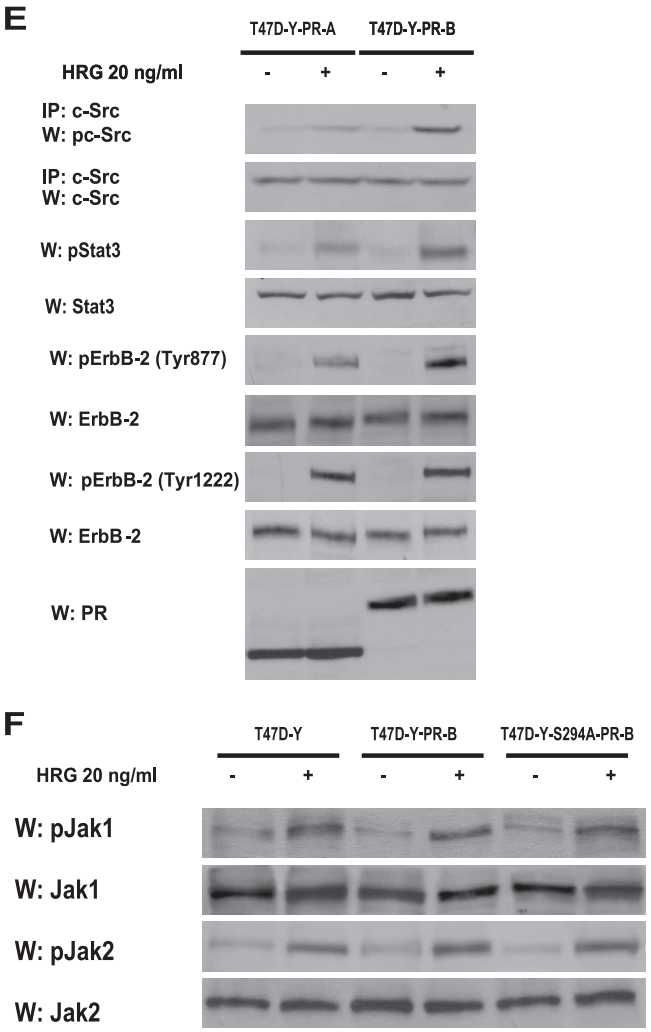

FIG. 6. PR and c-Src roles as upstream activators of ErbB-2. (A) C4HD cells were pretreated with RU486 or UO126 and were also transfected with PR or control siRNA before 10 min of HRG treatment. ErbB-2 activation was studied as described in the legend to Fig. 3, and data analysis showed significant ($P < 0.001$) inhibition of ErbB-2 total tyrosine phosphorylation levels by RU486, UO126, and PR siRNA. (B) C4HD cells were treated as described for panel A, protein extracts were electrophoresed (50 μg), and Western blots were performed with ErbB-2 tyrosine 877/927 and 1222/1272 or total ErbB-2 antibodies. Phospho-ErbB-2 bands were subjected to densitometry, and values were normalized to total protein bands, showing that the HRG-induced increase in ErbB-2 phosphorylation on the indicated tyrosines compared with that in untreated cells, the PP2, RU486, UO126, and PR siRNA inhibition of HRG-induced phosphorylation of ErbB-2 on Tyr 927, and the PP2 abolishment of HRG-stimulated ErbB-2 phosphorylation on Tyr 1272 were significant ($P < 0.001$). (C) The indicated cells were stimulated with HRG and studied for levels of ErbB-2 phosphorylation on specific residues as detailed for panel B. (D) Protein extracts (1 mg) from cells treated and not treated with HRG for 10 min and preincubated with UO126 before HRG stimulation were immunoprecipitated with an ErbB-2 antibody and analyzed by Western blotting with PR and c-Src antibodies. As a control, lysates were also immunoprecipitated with NRS. (E) The indicated cells were treated with HRG for 10 min or left untreated. Protein extracts were electrophoresed (50 μg), and Western blots were performed with antibodies to the phosphorylated forms of Stat3 and ErbB-2. Filters were stripped and reprobed with total Stat3 or ErbB-2 antibody. c-Src activity was studied as described in the legend to Fig. 1. Phospho-protein bands underwent densitometry, and values were normalized to total protein bands. Data analysis showed that the HRG-induced levels of Stat3, c-Src, and Tyr 877 ErbB-2 phosphorylation in T47D-Y-PR-B cells were significantly higher than the levels in T47D-Y-PR-A cells ($P < 0.001$). Controls for PR isoform expression are shown in the lower panel. The experiment shown was repeated three times. W, Western blot; IP, immunoprecipitation. (F) The indicated cell types were treated with HRG for 10 min or remained untreated, and Jak activity was determined as described in the legend to Fig. 1. Phospho-Jak bands underwent densitometry, and values were normalized to total protein bands. Data analysis showed that the increase in Jak phosphorylation in cells treated with HRG compared with that in untreated cells was significant ($P < 0.001$). The experiment shown was repeated three times with similar results. W, Western blot.

trastingly, similar levels of ErbB-2 phosphorylation at Tyr 1222/1272 were found in both cell types (Fig. 6E), consistent with our findings evidencing that HRG stimulates the phosphorylation of this carboxy-terminal residue independently of PR expression (Fig. 6C). These results indicate a differential PR-A capacity to interact with signaling pathways for cells stimulated with HRG compared to those for cells stimulated with progestins.

Since our findings revealed that ErbB-2 and c-Src act hierarchically as upstream Jak activators (Fig. 2B), we explored whether full PR-mediated ErbB-2 and c-Src phosphorylation is required for HRG-induced Jak activation. As shown in Fig. 6F, HRG was able to induce Jak activation in T47D-Y, T47D-Y-PR-B, and T47D-Y-S294A-PR-B cells.

To further demonstrate that c-Src-mediated phosphorylation of ErbB-2 on Tyr 877 is the key event that leads to Stat3 activation, we used another experimental model, human breast cancer SK-BR-3 cells, which overexpress ErbB-2 and lack PR (24). We found that SK-BR-3 cells display high levels of ErbB-2 Tyr 877 and Tyr 1222 phosphorylation and that HRG treatment for 10 min did not regulate the ErbB-2 phosphorylation state of any of these residues (Fig. 7). As previously reported (31), we found constitutive Tyr 705 Stat3 phosphorylation in these cells, as well as c-Src activation (Fig. 7). As happened in C4HD and T47D cells, c-Src inhibition with PP2 resulted in strong abrogation of ErbB-2 Tyr 877 phosphorylation but only slightly reduced Tyr 1222 phosphorylation levels in SK-BR-3 cells (Fig. 7). Abolishment of ErbB-2 Tyr 877 phosphorylation resulted in a strong decrease in the level of Stat3 phosphorylation, clearly showing the requirement of this specific ErbB-2 phosphorylation for Stat3 activation (Fig. 7). Among the Src family kinases, Fyn and Yes are also present in cells with ErbB-2 expression (37), which theoretically raises the possibility that they participate in the signaling described here. However, it is notable that the Fyn SH3 domain has been shown not to associate with PR (5), which would, in principle, preclude its involvement.

HRG induces Stat3 transcriptional activation through an ErbB-2-, ErbB-3-, Jak1-, Jak2-, Src-, and PR-dependent pathway. We then explored the effects of HRG on Stat3 transcriptional activation. C4HD cells were transiently transfected with a luciferase reporter plasmid containing four copies of the m67 high-affinity binding site (7) and with a plasmid encoding *Renilla* luciferase as an internal control. Treatment of C4HD cells with HRG induced Stat3 transcriptional activation that was completely inhibited by abrogation of ErbB-2 expression and

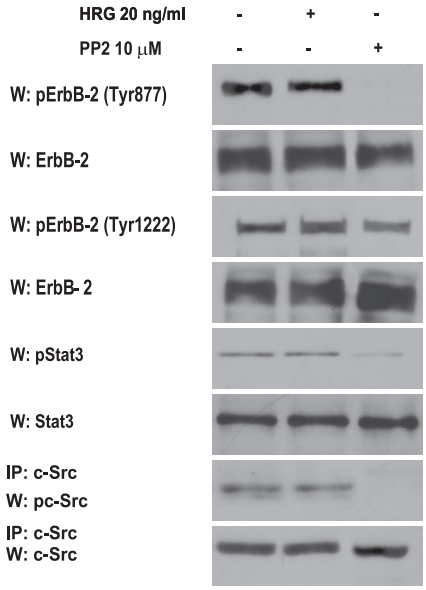

FIG. 7. ErbB-2 Tyr 877 phosphorylation is required for Stat3 activity. SK-BR-3 cells were treated or not treated with HRG for 10 min or were incubated with PP2. ErbB-2 phosphorylation was studied as described in the legend to Fig. 6B, and Stat3 and c-Src phosphorylation was studied as described in the legend to Fig. 1. Phospho-protein bands underwent densitometry, and values were normalized to total protein bands. Data analysis showed that the inhibition of ErbB-2 Tyr 877 phosphorylation and Stat3 activation by PP2 was significant ($P < 0.001$). The experiment shown was repeated three times. W, Western blot; IP, immunoprecipitation.

of ErbB-3 activation (Fig. 8A). Blockage of Src, Jak1, and Jak2 activities also inhibited HRG capacity to activate the m67-Luc reporter plasmid (Fig. 8A), as did preincubation of C4HD cells with RU486 (Fig. 8A). We also examined HRG capacity to induce Stat3 transcriptional activation in T47D cells that we engineered to stably express a luciferase gene construct under the control of a Stat3-specific promoter (T47D-Luc). Our results revealed that HRG was able to induce Stat3 transcriptional activation in these cells by the same mechanisms as those in C4HD cells (Fig. 8B).

Stat3 activity is a requisite in HRG-induced proliferation of C4HD and T47D cells. To investigate the correlation between HRG-induced Stat3 activation and cell growth, C4HD cells were transiently transfected with a DN Stat3 expression vector, Stat3Y705-F (6). We also examined the effects of Stat3 protein knockdown, using four different siRNA sequences targeting endogenous Stat3. Proliferation of transfected C4HD cells was evaluated by incorporation of [^{3}H]thymidine. As we previously reported (2), HRG was able to induce a potent proliferative response on C4HD cells (Fig. 9A). Expression of the Stat3Y705-F mutant had an inhibitory effect on HRG-induced growth of C4HD cells compared with that of HRG-stimulated C4HD cells transfected with the empty vector (Fig. 9A). Silencing Stat3 expression with all four Stat3 siRNAs also significantly inhibited HRG-stimulated proliferation. The results shown in Fig. 9A were obtained with two of the siRNAs employed. Controls for Stat3 protein expression inhibition by the two siRNAs used are shown in Fig. S5A in the supplemental material. The expression, function, and specificity of the Stat3Y705-F plasmid under the conditions described above, in which it modulates C4HD cell growth, are also shown in Fig. S5B to D in the supplemental material. Proliferation of transfected C4HD cells was also evaluated by PI staining and flow cytometry analysis. As shown in Fig. 9B, knockdown of Stat3 expression with Stat3 siRNA-1 had an inhibitory effect on HRG-induced growth of C4HD cells compared with that of C4HD cells transfected with control siRNA or of untreated wild-type C4HD cells. We have also already shown that HRG stimulates proliferation of T47D cells (2). Our present findings demonstrate that Stat3 activation is an absolute requirement

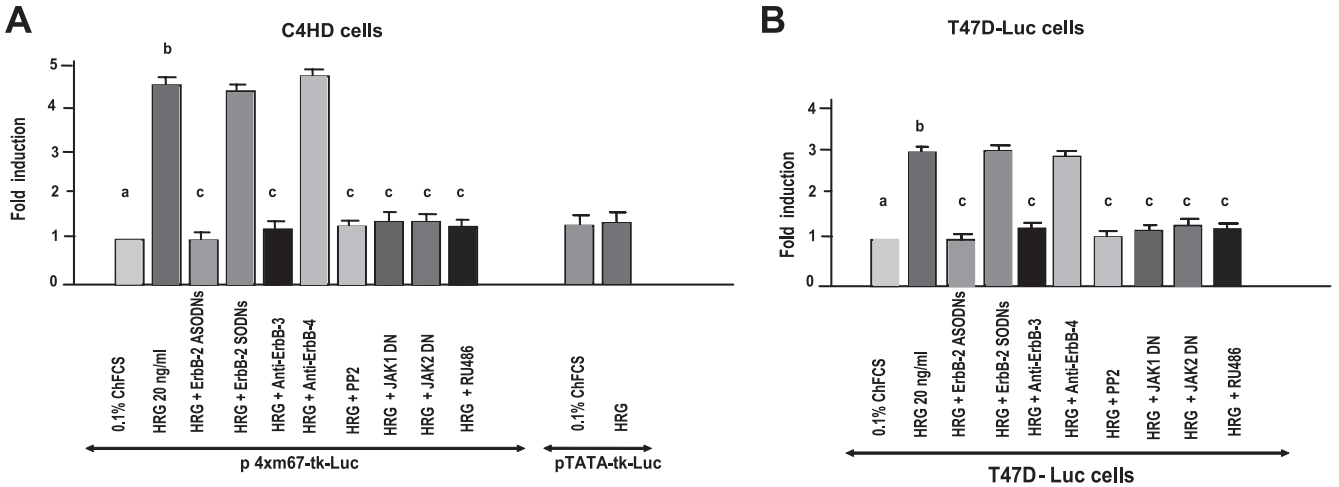

FIG. 8. HRG induces Stat3 transcriptional activation. (A) C4HD cells were transiently transfected with a luciferase reporter plasmid containing the m67 high-affinity binding site and with a plasmid encoding *Renilla* luciferase. Cells were pretreated with the indicated inhibitors, ODNs, or antibodies or cotransfected with the DN Jak1 and DN Jak2 expression vectors. Cells were also transfected with a pTATA-tk-Luc reporter lacking the m67 insertion. After transfection, cells were treated with HRG for 48 h or were left untreated growing in medium with 0.1% ChFCS. (B) T47D cells engineered to stably express the luciferase gene construct under the control of a Stat3-specific promoter (T47D-Luc) were treated as described for panel A. Results are presented as the induction of luciferase activity with respect to that in cells growing in ChFCS. The data shown represent the mean of six independent experiments for each cell type ± the standard error of the mean ($P < 0.001$ for b versus a and c versus b).

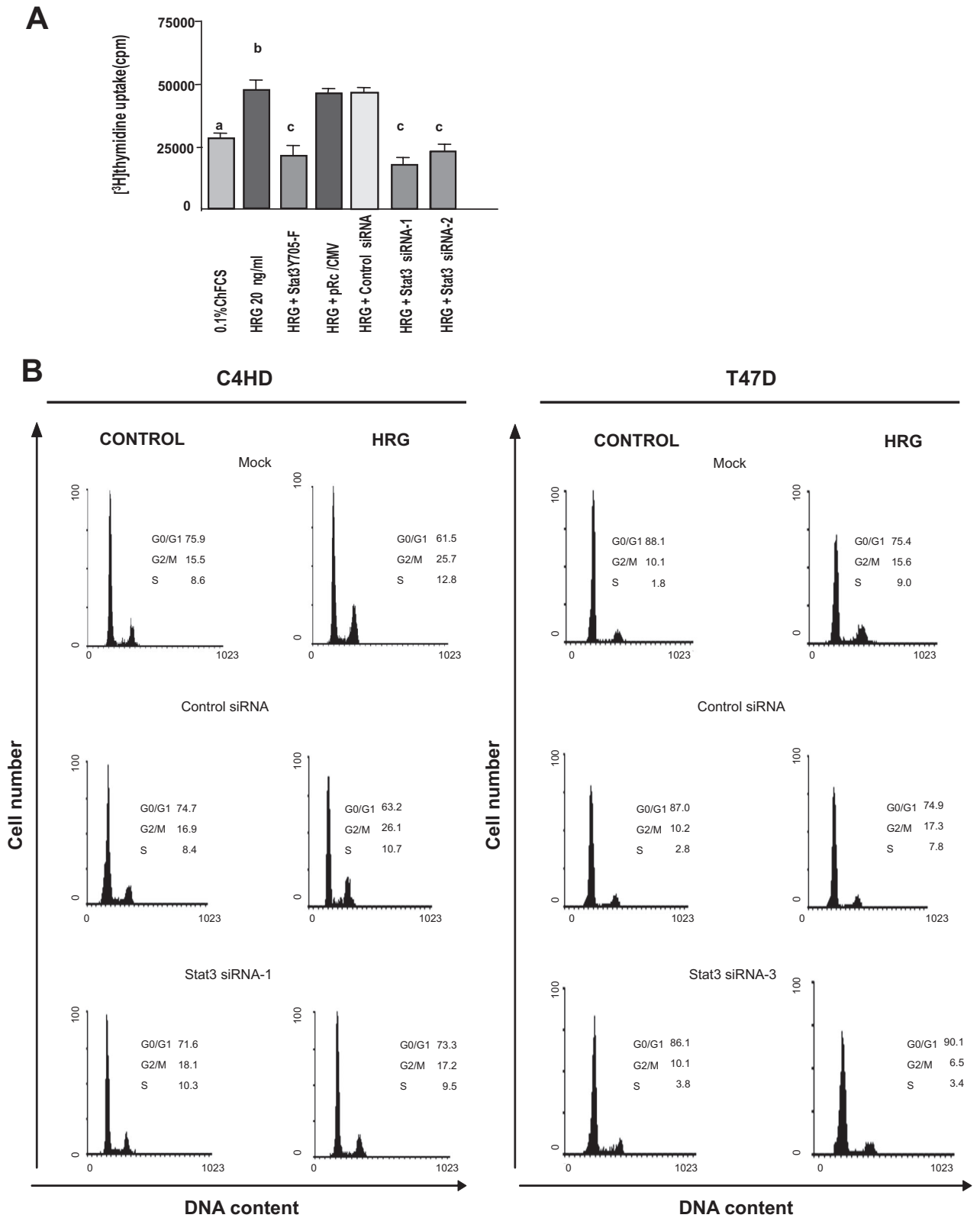

FIG. 9. Stat3 involvement in breast cancer proliferation in vitro. (A) C4HD cells were transiently transfected with the Stat3Y705-F vector, with the empty pRc/CMV vector, or with siRNAs before HRG treatment for 48 h. Incorporation of [^{3}H]thymidine was used as a measure of DNA synthesis. Data are presented as means ± standard deviations ($P < 0.001$ for b versus a and c versus b). The experiment shown is representative of a total of three. (B) C4HD and T47D cells were transfected with the indicated siRNAs before HRG treatment for 48 h and were then stained with PI and analyzed for cell cycle distribution by flow cytometry. The percentages of total cells in the cell cycle phases are indicated. Mock, cells incubated with the transfection reagent. The experiments shown are representative of a total of three.

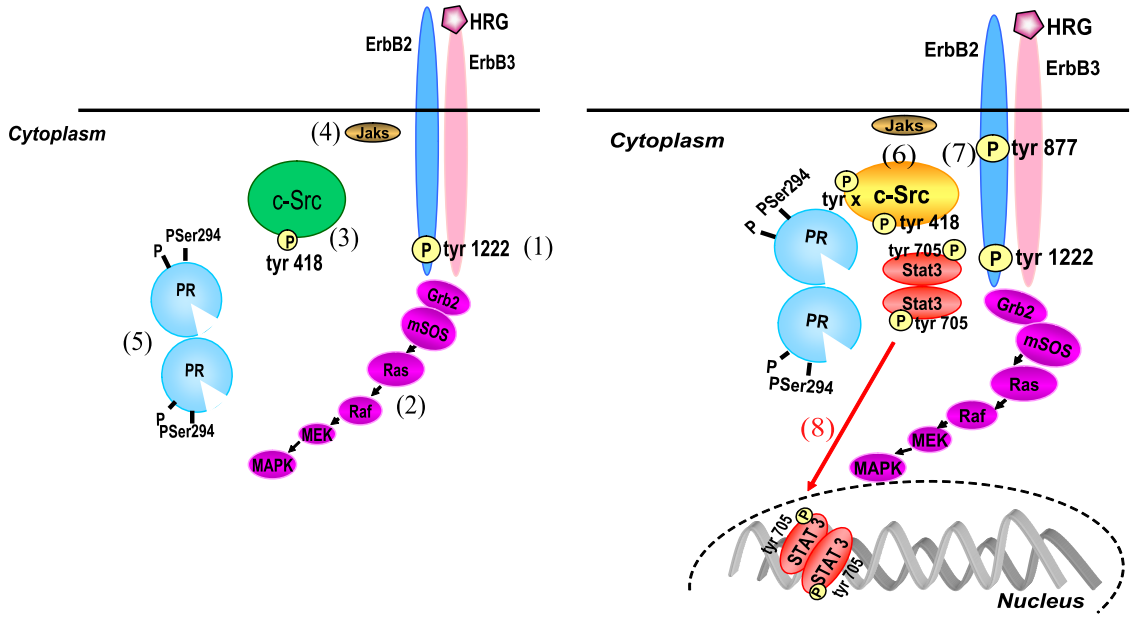

FIG. 10. Model of HRG/ErbB-2-induced Stat3 activation. HRG binding induces ErbB-2/ErbB-3 heterodimerization and the concomitant phosphorylation of ErbB-2 at the Tyr 1222 autophosphorylation site (1), which couples ErbB-2 to the MAPK cascade (2). On the other hand, HRG stimulates a first level of c-Src activation through a PR-independent mechanism (3). Jaks are also activated independently of PR (4). HRG-activated p42/p44 MAPKs induce the rapid phosphorylation of PR on Ser 294 (5). PR phosphorylated on Ser 294 then promotes a second round of c-Src activation (6). c-Src, dually activated firstly by ErbB-2 acting as an upstream effector and then by HRG-activated PR, acts in turn as an upstream modulator of ErbB-2 and induces its phosphorylation on Tyr 877 (7), with the latter being the molecular event that couples HRG/ErbB-2 to Stat3 activation (8).

for the mechanism of HRG-induced T47D cell proliferation (Fig. 9B). A control for the effect of siRNA-3 in T47D cells is shown in Fig. S5A in the supplemental material.

DISCUSSION

The present study offers novel mechanistic insight into the interaction of SHR and ErbBs in breast cancer, highlighting the notion that HRG/ErbB-2 activates Stat3 through the co-option of PR signaling. Activated Stat3 in turn acts as a downstream effector of both HRG/ErbB-2 and unliganded PR to induce proliferation of mammary tumors.

We have identified the molecular mechanism involved in HRG stimulation of Stat3 activity in mouse C4HD and human T47D breast cancer cells. We provide evidence, firstly, that the HRG effects on Stat3 tyrosine phosphorylation require both functional ErbB-2 and ErbB-3. Our results also demonstrate that HRG activates Jak1, Jak2, and c-Src in C4HD and T47D cells and that all three participate in HRG-induced Stat3 tyrosine phosphorylation through a mechanism in which ErbB-2 and c-Src act hierarchically upstream of Jaks. In addition, we found a bidirectional interplay between ErbB-2 and c-Src in HRG-stimulated activation of these kinases in C4HD and T47D cells. As previously described (19), our findings evidenced that c-Src activation is dependent on ErbB-2 in both cell types. Notably, we found that c-Src also plays a role as an upstream activator of ErbB-2. Stat3 activity has been reported for models of constitutive ErbB-2 activation in Cos-7 and NIH 3T3 cells (30), similar to our present findings that ErbB-2 intrinsic tyrosine kinase activity, c-Src, and Jak2 are required to maintain Stat3 activation. The involvement of Stat3 and ErbB-2 in mammary tumorigenesis is well acknowledged, and the correlation between constitutively activated Stat3 and high levels of ErbB-2 expression has been found in breast tumor samples (12). However, our study is the first to report the effects of ligand-dependent ErbB-2 activation on Stat3 activity in breast cancer. Until now, studies with mammary tumor cells have shown two levels of Stat3 activation, namely, a constitutive Stat3 activation that depends on Src and Jaks but remains unaffected by inhibition of EGFR activity (29), and an EGF-inducible Stat3 activity that is abolished by blockage of EGFR and Jak activities (15, 23).

An exciting and novel finding of this study is that PR is a key player in HRG-induced Stat3 phosphorylation through its capacity to differentially modulate c-Src activation. We have revealed the coordinated responses involved in these multiple regulatory steps, and our results are consistent with the model shown in Fig. 10. Thus, we have identified a mechanism in which rapid MAPK activation occurs, as described previously (18), via HRG induction of ErbB-2/ErbB-3 heterodimerization, followed by the activation of ErbB-2 intrinsic tyrosine kinase and concomitant phosphorylation of ErbB-2 at the autophosphorylation sites within its carboxy-terminal region. Among these residues, we have identified Tyr 1222/1272 (Fig. 10, left panel, step 1), whose HRG-induced phosphorylation is independent of PR and can occur to a significant extent in the absence of c-Src activity, as reported for models of constitutive ErbB-2 activation (17). Interestingly, our result is the first demonstration of the capacity of HRG to induce ErbB-2 phosphorylation at a specific autophosphorylation site in breast cancer. Phosphorylated tyrosines have been found to couple

ErbB-2 to the MAPK cascade through a series of adaptor proteins that link autophosphorylated ErbB-2 to the Sos/p21ras/Raf/MEK/MAPK pathway (10, 11). Consistent with our present results, the participation of c-Src in this pathway has already been found (18). Our results for C4HD and T47D cells as well as reconstitution experiments with T47D-Y cells show that HRG capacity to induce rapid p42/p44 MAPK activation (Fig. 10, left panel, step 2) is also independent of PR expression, activation, or Ser 294 phosphorylation or the presence of an intact polyproline motif. These results are in agreement with startling findings evidencing that EGF induces strong activation of MAPKs in T47D-Y cells expressing both wild-type and mutant Ser294A PR-B (32).

Two levels of HRG-induced c-Src activation were found in our model systems. First, HRG was able to induce c-Src activation through a PR-independent mechanism. This is consistent with a model of direct c-Src activation in which ErbB-2, phosphorylated at tyrosine residues by HRG stimulation, physically associates with the SH2 domain of c-Src, allowing c-Src activation and Tyr 418/423 autophosphorylation (Fig. 10, left panel, step 3), as previously described (19). The positions of the ErbB-2 phosphorylated tyrosine residues that interact with c-Src remain to be elucidated. As mentioned above, phosphorylation of the Tyr 1222 carboxy-terminal site can occur in the absence of c-Src activity, indicating that this residue is phosphorylated by HRG upstream of c-Src. This raises the possibility of Tyr 1222 involvement in the association between ErbB-2 and c-Src, leading to the rapid, PR-independent HRG stimulation of c-Src phosphorylation. The roles of ErbB-2 and c-Src as upstream hierarchical activators of Jaks indicate that Jaks participate in Stat3 phosphorylation only after the two former proteins have been activated. Our present findings also indicate that full PR-mediated ErbB-2 or c-Src phosphorylation is not required for HRG-induced Jak activation. Consequently, we have presented Jaks at step 4 in Fig. 10 (left panel).

The second level of c-Src activation observed in our model systems requires PR expression, phosphorylation of PR on Ser 294 by HRG-activated p42/p44 MAPKs (Fig. 10, left panel, step 5), and the presence of an intact PR polyproline motif. Pioneering findings have demonstrated a direct interaction between PR-B and the SH3 domain of c-Src (5). Thus, the PR-dependent activation of c-Src (Fig. 10, right panel, step 6) found in our study could be explained for human PR by a mechanism in which PR interacts directly with c-Src by an SH3 domain displacement mechanism through the PR polyproline motif. Notably, we have also demonstrated for the first time that Ser 294 phosphorylation is another key regulatory modification of human PR function that leads to its association with and concomitant activation of c-Src. Mouse PR lacks the polyproline motif, which further highlights the importance of phosphorylation on specific residues, such as Ser 294, in PR regulation of c-Src activity.

Recent findings have demonstrated that c-Src acts as an upstream activator of ErbB-2 by promoting its phosphorylation at the Tyr 877 residue, which is different from the autophosphorylation sites and is located in the activation loop of the kinase domain (17, 37). Here we found that HRG induced ErbB-2 Tyr 877 phosphorylation in both C4HD and T47D cells, an effect that was completely blocked not only by PP2 but also by RU486 or UO126. These findings are consistent with a mechanism in which phosphorylation of ErbB-2 at Tyr 877 is induced by c-Src only when the latter is activated by unliganded PR phosphorylated at Ser 294 by HRG-activated MAPKs (Fig. 10, right panel, step 7). ErbB-2 Tyr 877 phosphorylation is thus the molecular event that couples HRG/ErbB-2 to Stat3 activation (Fig. 10, right panel, step 8). This finding is further supported by our results with SK-BR-3 cells revealing that ErbB-2 Tyr 877 phosphorylation is an absolute requirement for Stat3 activation. In summary, our results identified a mechanism in which c-Src, activated initially by the upstream effector ErbB-2 and then by PR, acts as the nodal convergence point between HRG-activated ErbB-2 and PR. Dually activated c-Src then becomes an upstream modulator of ErbB-2, inducing a differential phosphorylation of ErbB-2 that leads to Stat3 activation.

We have also revealed another aspect of PR biology in this study. Our findings with T47D-Y-PR-A cells showed that HRG is able to stimulate c-Src and Stat3 activation as well as ErbB-2 Tyr 877 phosphorylation. Although readily detected, the capacity of PR-A to modulate the activation of all three molecules upon HRG stimulation was significantly reduced compared to that of PR-B. A seminal study demonstrated the ability of PR-A to activate Src kinases in cell-free assays (5). However, PR-A-induced Src and MAPK activation in response to progestin within cells was highly reduced compared to that induced by PR-B (3, 4). The predominant localization of unliganded PR-A in the nucleus, which prevents its interaction with cytoplasmic signaling molecules, appears to account for this difference (3, 4). Our present findings disclose a differential PR-A capacity to interact with signaling pathways in response to HRG versus progestin. The distinct mechanisms, kinetics, and strength of signaling pathway activation induced by growth factors in comparison to progestins may explain this difference. For example, it was previously shown that EGF induced a stronger and more prolonged activation of MAPKs in breast cancer cells than progestins did (9, 14). Similarly, we found that compared to MPA, HRG induced significantly higher levels of MAPK activation in C4HD cells (data not shown). Therefore, rapid, strong, and sustained HRG-stimulated MAPK activation could result in a rapid increase of Ser 294 phosphorylation in the fraction of unliganded PR-A present in the cytoplasmic compartment, allowing PR-A interaction with c-Src, as we found in this study. A distinct modulation of the subcellular localization of PR by HRG relative to progestin may also contribute to the capacity of PR-A to activate signaling pathways. Indeed, it has been found that after 30 min of EGF treatment, the majority of PR-B still remains in the cytoplasmic fraction (9).

A recent study with a mutationally activated ErbB-2 mouse model of mammary cancer (Neu-β4-1355T) (17) showed that ErbB-2 induces phosphorylation of the β4 integrin signaling domain through a Src family kinase to promote tumor growth. On the other hand, inhibition of Src family kinases abolished ErbB-2 Tyr 877 phosphorylation in cells with an intact β4 integrin signaling domain. Similarly, deletion of the β4 integrin signaling domain resulted in abrogation of ErbB-2 Tyr 877 phosphorylation. In our model systems, PR plays essentially the same role as β4 integrin. Thus, PR is both a downstream target of ErbB-2, which phosphorylates PR through HRG-activated MAPKs,

and an upstream activator of ErbB-2 through its capacity to induce c-Src activation leading to phosphorylation of ErbB-2 at Tyr 877. Comparable to our present findings, deletion of the β4 signaling domain impairs Stat3 activation induced by constitutively activated ErbB-2 (17).

Finally, we found that Stat3 is a key player in HRG-induced C4HD cell growth. These findings, which provide the first evidence that Stat3 participates in HRG-induced breast cancer growth, are in line with the accumulating evidence demonstrating the involvement of Stat3 in the proliferation of breast cancer cells (8, 15, 16, 23). Our present work identifies two novel potential therapeutic interventions for PR- and ErbB-2-positive breast tumors. The first involves the specific blockage of PR signaling activity. The second proposes that targeting Stat3 could become a valuable alternative therapy for a more effective treatment of breast cancers that are resistant to first-line antihormonal and second-line anti-tyrosine-kinase therapies, such as blockage of ErbB-2 activity.

ACKNOWLEDGMENTS

This work was supported by grants IDB 1728 OC/AR PICT 25301 (2004) and 0211 (2006) from the National Agency of Scientific Promotion of Argentina and PIP 5391 from the Argentina National Council of Scientific Research, all awarded to P.V.E., and Oncomed-Reno CONICET 1819/03, from the Henry Moore Institute of Argentina (P.V.E. and R.S.).

We thank A. A. Molinolo (NIH, Bethesda, MD) for his generous and constant help and support, K. Horwitz (University of Colorado) for the gift of the T47D-Y cell line and the hPR expression vector, C. Lange (University of Minnesota) for providing the S294A mutant PR-B, D. Edwards (Baylor College of Medicine) for the gift of the mutant PR-BmPro, E. Bal de Kier Joffe (Roffo Institute, Buenos Aires, Argentina) for her helpful discussions and critical reading of the manuscript, and C. Lanari (IBYME, Buenos Aires, Argentina) for providing the MPA-induced mammary tumor model.

REFERENCES

1. **Balana, M. E., L. Labriola, M. Salatino, F. Movsichoff, G. Peters, E. H. Charreau, and P. V. Elizalde.** 2001. Activation of ErbB-2 via a hierarchical interaction between ErbB-2 and type I insulin-like growth factor receptor in mammary tumor cells. Oncogene **20:**34–47.
2. **Balana, M. E., R. Lupu, L. Labriola, E. H. Charreau, and P. V. Elizalde.** 1999. Interactions between progestins and heregulin (HRG) signaling pathways: HRG acts as mediator of progestins proliferative effects in mouse mammary adenocarcinomas. Oncogene **18:**6370–6379.
3. **Boonyaratanakornkit, V., Y. Bi, M. Rudd, and D. P. Edwards.** 2008. The role and mechanism of progesterone receptor activation of extra-nuclear signaling pathways in regulating gene transcription and cell cycle progression. Steroids **73:**922–928.
4. **Boonyaratanakornkit, V., E. McGowan, L. Sherman, M. A. Mancini, B. J. Cheskis, and D. P. Edwards.** 2007. The role of extranuclear signaling actions of progesterone receptor in mediating progesterone regulation of gene expression and the cell cycle. Mol. Endocrinol. **21:**359–375.
5. **Boonyaratanakornkit, V., M. P. Scott, V. Ribon, L. Sherman, S. M. Anderson, J. L. Maller, W. T. Miller, and D. P. Edwards.** 2001. Progesterone receptor contains a proline-rich motif that directly interacts with SH3 domains and activates c-Src family tyrosine kinases. Mol. Cell **8:**269–280.
6. **Bromberg, J. F., C. M. Horvath, D. Besser, W. W. Lathem, and J. E. Darnell, Jr.** 1998. Stat3 activation is required for cellular transformation by v-src. Mol. Cell. Biol. **18:**2553–2558.
7. **Bromberg, J. F., M. H. Wrzeszczynska, G. Devgan, Y. Zhao, R. G. Pestell, C. Albanese, and J. E. Darnell, Jr.** 1999. Stat3 as an oncogene. Cell **98:**295–303.
8. **Burke, W. M., X. Jin, H. J. Lin, M. Huang, R. Liu, R. K. Reynolds, and J. Lin.** 2001. Inhibition of constitutively active Stat3 suppresses growth of human ovarian and breast cancer cells. Oncogene **20:**7925–7934.
9. **Daniel, A. R., M. Qiu, E. J. Faivre, J. H. Ostrander, A. Skildum, and C. A. Lange.** 2007. Linkage of progestin and epidermal growth factor signaling: phosphorylation of progesterone receptors mediates transcriptional hypersensitivity and increased ligand-independent breast cancer cell growth. Steroids **72:**188–201.
10. **Dankort, D., N. Jeyabalan, N. Jones, D. J. Dumont, and W. J. Muller.** 2001. Multiple ErbB-2/Neu phosphorylation sites mediate transformation through distinct effector proteins. J. Biol. Chem. **276:**38921–38928.
11. **Dankort, D., B. Maslikowski, N. Warner, N. Kanno, H. Kim, Z. Wang, M. F. Moran, R. G. Oshima, R. D. Cardiff, and W. J. Muller.** 2001. Grb2 and Shc adapter proteins play distinct roles in Neu (ErbB-2)-induced mammary tumorigenesis: implications for human breast cancer. Mol. Cell. Biol. **21:**1540–1551.
12. **Diaz, N., S. Minton, C. Cox, T. Bowman, T. Gritsko, R. Garcia, I. Eweis, M. Wloch, S. Livingston, E. Seijo, A. Cantor, J. H. Lee, C. A. Beam, D. Sullivan, R. Jove, and C. A. Muro-Cacho.** 2006. Activation of stat3 in primary tumors from high-risk breast cancer patients is associated with elevated levels of activated SRC and survivin expression. Clin. Cancer Res. **12:**20–28.
13. **Dran, G., I. A. Luthy, A. A. Molinolo, F. Montecchia, E. H. Charreau, C. D. Pasqualini, and C. Lanari.** 1995. Effect of medroxyprogesterone acetate (MPA) and serum factors on cell proliferation in primary cultures of an MPA-induced mammary adenocarcinoma. Breast Cancer Res. Treat. **35:**173–186.
14. **Faivre, E. J., A. R. Daniel, C. J. Hillard, and C. A. Lange.** 2008. Progesterone receptor rapid signaling mediates serine 345 phosphorylation and tethering to specificity protein 1 transcription factors. Mol. Endocrinol. **22:**823–837.
15. **Garcia, R., T. L. Bowman, G. Niu, H. Yu, S. Minton, C. A. Muro-Cacho, C. E. Cox, R. Falcone, R. Fairclough, S. Parsons, A. Laudano, A. Gazit, A. Levitzki, A. Kraker, and R. Jove.** 2001. Constitutive activation of Stat3 by the Src and JAK tyrosine kinases participates in growth regulation of human breast carcinoma cells. Oncogene **20:**2499–2513.
16. **Gritsko, T., A. Williams, J. Turkson, S. Kaneko, T. Bowman, M. Huang, S. Nam, I. Eweis, N. Diaz, D. Sullivan, S. Yoder, S. Enkemann, S. Eschrich, J. H. Lee, C. A. Beam, J. Cheng, S. Minton, C. A. Muro-Cacho, and R. Jove.** 2006. Persistent activation of stat3 signaling induces survivin gene expression and confers resistance to apoptosis in human breast cancer cells. Clin. Cancer Res. **12:**11–19.
17. **Guo, W., Y. Pylayeva, A. Pepe, T. Yoshioka, W. J. Muller, G. Inghirami, and F. G. Giancotti.** 2006. Beta 4 integrin amplifies ErbB2 signaling to promote mammary tumorigenesis. Cell **126:**489–502.
18. **Ishizawar, R. C., T. Miyake, and S. J. Parsons.** 2007. c-Src modulates ErbB2 and ErbB3 heterocomplex formation and function. Oncogene **26:**3503–3510.
19. **Kim, H., R. Chan, D. L. Dankort, D. Zuo, M. Najoukas, M. Park, and W. J. Muller.** 2005. The c-Src tyrosine kinase associates with the catalytic domain of ErbB-2: implications for ErbB-2 mediated signaling and transformation. Oncogene **24:**7599–7607.
20. **Labriola, L., M. Salatino, C. J. Proietti, A. Pecci, O. A. Coso, A. R. Kornblihtt, E. H. Charreau, and P. V. Elizalde.** 2003. Heregulin induces transcriptional activation of the progesterone receptor by a mechanism that requires functional ErbB-2 and mitogen-activated protein kinase activation in breast cancer cells. Mol. Cell. Biol. **23:**1095–1111.
21. **Lange, C. A., J. K. Richer, T. Shen, and K. B. Horwitz.** 1998. Convergence of progesterone and epidermal growth factor signaling in breast cancer. Potentiation of mitogen-activated protein kinase pathways. J. Biol. Chem. **273:**31308–31316.
22. **Lange, C. A., T. Shen, and K. B. Horwitz.** 2000. Phosphorylation of human progesterone receptors at serine-294 by mitogen-activated protein kinase signals their degradation by the 26S proteasome. Proc. Natl. Acad. Sci. USA **97:**1032–1037.
23. **Li, L., and P. E. Shaw.** 2002. Autocrine-mediated activation of STAT3 correlates with cell proliferation in breast carcinoma lines. J. Biol. Chem. **277:**17397–17405.
24. **Lupu, R., R. B. Dickson, and M. E. Lippman.** 1992. The role of erbB-2 and its ligands in growth control of malignant breast epithelium. J. Steroid Biochem. Mol. Biol. **43:**229–236.
25. **Migliaccio, A., D. Piccolo, G. Castoria, M. Di Domenico, A. Bilancio, M. Lombardi, W. Gong, M. Beato, and F. Auricchio.** 1998. Activation of the Src/p21ras/Erk pathway by progesterone receptor via cross-talk with estrogen receptor. EMBO J. **17:**2008–2018.
26. **Olayioye, M. A., I. Beuvink, K. Horsch, J. M. Daly, and N. E. Hynes.** 1999. ErbB receptor-induced activation of stat transcription factors is mediated by Src tyrosine kinases. J. Biol. Chem. **274:**17209–17218.
27. **Olayioye, M. A., R. M. Neve, H. A. Lane, and N. E. Hynes.** 2000. The ErbB signaling network: receptor heterodimerization in development and cancer. EMBO J. **19:**3159–3167.
28. **Proietti, C., M. Salatino, C. Rosemblit, R. Carnevale, A. Pecci, A. R. Kornblihtt, A. A. Molinolo, I. Frahm, E. H. Charreau, R. Schillaci, and P. V. Elizalde.** 2005. Progestins induce transcriptional activation of signal transducer and activator of transcription 3 (Stat3) via a Jak- and Src-dependent mechanism in breast cancer cells. Mol. Cell. Biol. **25:**4826–4840.
29. **Real, P. J., A. Sierra, A. De Juan, J. C. Segovia, J. M. Lopez-Vega, and J. L. Fernandez-Luna.** 2002. Resistance to chemotherapy via Stat3-dependent overexpression of Bcl-2 in metastatic breast cancer cells. Oncogene **21:**7611–7618.

30. **Ren, Z., and T. S. Schaefer.** 2002. ErbB-2 activates Stat3 alpha in a Src- and JAK2-dependent manner. J. Biol. Chem. **277:**38486–38493.
31. **Sam, M. R., B. E. Elliott, and C. R. Mueller.** 2007. A novel activating role of SRC and STAT3 on HGF transcription in human breast cancer cells. Mol. Cancer **6:**69.
32. **Shen, T., K. B. Horwitz, and C. A. Lange.** 2001. Transcriptional hyperactivity of human progesterone receptors is coupled to their ligand-dependent down-regulation by mitogen-activated protein kinase-dependent phosphorylation of serine 294. Mol. Cell. Biol. **21:**6122–6131.
33. **Simian, M., A. Molinolo, and C. Lanari.** 2006. Involvement of matrix metalloproteinase activity in hormone-induced mammary tumor regression. Am. J. Pathol. **168:**270–279.
34. **Slamon, D. J., W. Godolphin, L. A. Jones, J. A. Holt, S. G. Wong, D. E. Keith, W. J. Levin, S. G. Stuart, J. Udove, and A. Ullrich.** 1989. Studies of the HER-2/neu proto-oncogene in human breast and ovarian cancer. Science **244:**707–712.
35. **Tzahar, E., H. Waterman, X. Chen, G. Levkowitz, D. Karunagaran, S. Lavi, B. J. Ratzkin, and Y. Yarden.** 1996. A hierarchical network of interreceptor interactions determines signal transduction by Neu differentiation factor/neuregulin and epidermal growth factor. Mol. Cell. Biol. **16:**5276–5287.
36. **Wang, S. C., H. C. Lien, W. Xia, I. F. Chen, H. W. Lo, Z. Wang, M. Ali-Seyed, D. F. Lee, G. Bartholomeusz, F. Ou-Yang, D. K. Giri, and M. C. Hung.** 2004. Binding at and transactivation of the COX-2 promoter by nuclear tyrosine kinase receptor ErbB-2. Cancer Cell **6:**251–261.
37. **Xu, W., X. Yuan, K. Beebe, Z. Xiang, and L. Neckers.** 2007. Loss of Hsp90 association up-regulates Src-dependent ErbB2 activity. Mol. Cell. Biol. **27:**220–228.
38. **Yu, H., and R. Jove.** 2004. The STATs of cancer—new molecular targets come of age. Nat. Rev. Cancer **4:**97–105.
39. **Zhang, Y., W. Bai, V. E. Allgood, and N. L. Weigel.** 1994. Multiple signaling pathways activate the chicken progesterone receptor. Mol. Endocrinol. **8:**577–584.